



Review

# Chromite Composition and Platinum-Group Elements Distribution in Tethyan Chromitites of the Mediterranean Basin: An Overview

Federica Zaccarini <sup>1,\*</sup>, Maria Economou-Eliopoulos <sup>2</sup> , Basilios Tsikouras <sup>1</sup>  and Giorgio Garuti <sup>1</sup>

<sup>1</sup> Geosciences Programme, Faculty of Science, Universiti Brunei Darussalam, Jalan Tungku Link, Gadong, Bandar Seri Begawan BE1410, Brunei; basilios.tsikouras@ubd.edu.bn (B.T.); giorgio.garuti1945@gmail.com (G.G.)

<sup>2</sup> Department of Geology and Geoenvironment, University of Athens, 15784 Athens, Greece; econom@geol.uoa.gr

\* Correspondence: federicazaccarinigaruti@gmail.com; Tel.: +43-664-3868590

**Abstract:** This study provides a comprehensive literature review of the distribution, the platinum-group elements (PGE) composition, and mineral chemistry of chromitites associated with Mesozoic Tethyan ophiolites in the Mediterranean Basin. These suites outcrop in the northern Italian Apennines, the Balkans, Turkey, and Cyprus. Most chromitites occur in depleted mantle tectonites, with fewer found in the mantle-transition zone (MTZ) and supra-Moho cumulates. Based on their  $Cr\# = (Cr / (Cr + Al))$  values, chromitites are primarily classified as high-Cr, with a subordinate presence of high-Al chromitites. Occasionally, high-Al and high-Cr chromitites co-exist within the same ophiolite complex. High-Cr chromitites are formed in supra-subduction zone (SSZ) environments, where depleted mantle interacts with high-Mg boninitic melts. Conversely, high-Al chromitites are typically associated with extensional tectonic regimes and more fertile peridotites. The co-existence of high-Al and high-Cr chromitites within the same ophiolite is attributed to tectonic movements and separate magma intrusions from variably depleted mantle sources, such as mid-ocean ridge basalts (MORB) and back-arc basin basalts. These chromitites formed in different geodynamic settings during the transition of the oceanic lithosphere from a mid-ocean ridge (MOR) to a supra-subduction zone (SSZ) regime or, alternatively, within an SSZ during the differentiation of a single boninitic magma batch. Distinct bimodal distribution and vertical zoning were observed: high-Cr chromitites formed in the deep mantle, while Al-rich counterparts formed at shallower depths near the MTZ. Only a few of the aforementioned chromitites, particularly the high-Cr ones, are enriched in the refractory IPGE (iridium-group PGE: Os, Ir, Ru) relative to PPGE (palladium-group PGE: Rh, Pt, Pd), with an average PPGE/IPGE ratio of 0.66, resulting in well-defined negative slopes in PGE patterns. The IPGE enrichment is attributed to their compatible geochemical behavior during significant degrees of partial melting (up to 30%) of the host mantle. It is suggested that the boninitic melt, which crystallized the high-Cr chromitites, was enriched in IPGE during melt-rock reactions with the mantle source, thus enriching the chromitites in IPGE as well. High-Al chromitites generally exhibit high PPGE/IPGE ratios, up to 3.14, and strongly fractionated chondrite-normalized PGE patterns with positive slopes and significant enrichments in Pt and Pd. The PPGE enrichment in high-Al chromitites is attributed to the lower degree of partial melting of their mantle source and crystallization from a MOR-type melt, which contains fewer IPGE than the boninitic melt above. High-Al chromitites forming at higher stratigraphic levels in the host ophiolite likely derive from progressively evolving parental magma. Thus, the PPGE enrichment in high-Al chromitites is attributed to crystal fractionation processes that consumed part of the IPGE during the early precipitation of co-existing high-Cr chromitites in the deep mantle. Only a few high-Al chromitites show PPGE enrichment due to local sulfur saturation and the potential formation of an immiscible sulfide liquid, which could concentrate the remaining PPGE in the ore-forming system.

**Keywords:** chromitite; Tethyan ophiolites; platinum-group elements; Mediterranean Basin



**Citation:** Zaccarini, F.; Economou-Eliopoulos, M.; Tsikouras, B.; Garuti, G. Chromite Composition and Platinum-Group Elements Distribution in Tethyan Chromitites of the Mediterranean Basin: An Overview. *Minerals* **2024**, *14*, 744. <https://doi.org/10.3390/min14080744>

Academic Editor: Alexandre V. Andronikov

Received: 29 June 2024

Revised: 16 July 2024

Accepted: 22 July 2024

Published: 24 July 2024



**Copyright:** © 2024 by the authors. Licensee MDPI, Basel, Switzerland. This article is an open access article distributed under the terms and conditions of the Creative Commons Attribution (CC BY) license (<https://creativecommons.org/licenses/by/4.0/>).

## 1. Introduction

Chromite, an oxide belonging to the spinel supergroup minerals, is the only commercial source of chromium. Chromium is essential in metallurgy, the refractory and glass industries, and various military applications, making it an important strategic metal. Economic chromite deposits are found in different types of ultramafic rocks, forming stratiform and podiform chromitites. Stratiform chromitites occur as massive and multiple layers, typically associated with the ultramafic portions of mafic–ultramafic layered intrusions emplaced in stable cratonic settings or during rift-related events, predominantly in the Precambrian [1]. The Bushveld Complex in South Africa, containing most of the world’s chromite reserves, is a prime example of a stratiform chromite deposit [2]. Podiform chromitites, on the other hand, are found in the mantle sections of ophiolite complexes. Their host rocks are variably serpentinized peridotites, mainly harzburgite. Podiform chromitites are the second most significant natural source of chromite for industrial use, with the most typical examples occurring in the giant Kempirsai deposit in Kazakhstan and numerous smaller deposits in Turkey [3]. Chromitites also efficiently collect critical and high-priced PGE (Os, Ir, Ru, Rh, Pt, Pd). However, few stratiform chromitites contain economically viable amounts of PGE; the only currently mined example is the Upper Group 2 (UG2) stratiform chromitite of the Bushveld Igneous Complex in South Africa [4]. The distribution of PGE in podiform chromitites is influenced by factors such as the fertility of the mantle source, the fractional crystallization of the parent melt, and the presence of an immiscible sulfide liquid. Consequently, the chromite composition and PGE geochemistry of ophiolitic chromitites serve as significant petrogenetic indicators of mantle source characteristics and geodynamic settings [5–13]. The vast Tethyan belt, extending from western Europe to southeast Asia [5], is a world-class orogenic belt containing numerous ophiolitic fragments (Figure 1). Tethyan ophiolites in the Mediterranean Basin exhibit petrogenetic characteristics associated with extensional tectonic regimes, such as mid-oceanic ridges (MORs) spreading centers, compressive tectonic regimes, such as supra-subduction zones (SSZs), or regions transitional between MORs and SSZs [6–8]. Within a single complex, ophiolitic rocks with different geochemical characteristics can co-exist. Studies indicate that large-scale chromite deposits are mainly associated with SSZ ophiolites, typically located in mantle tectonites (harzburgite), whereas subeconomic chromite mineralization occurs in the supra-Moho cumulus sequence or MOR settings.

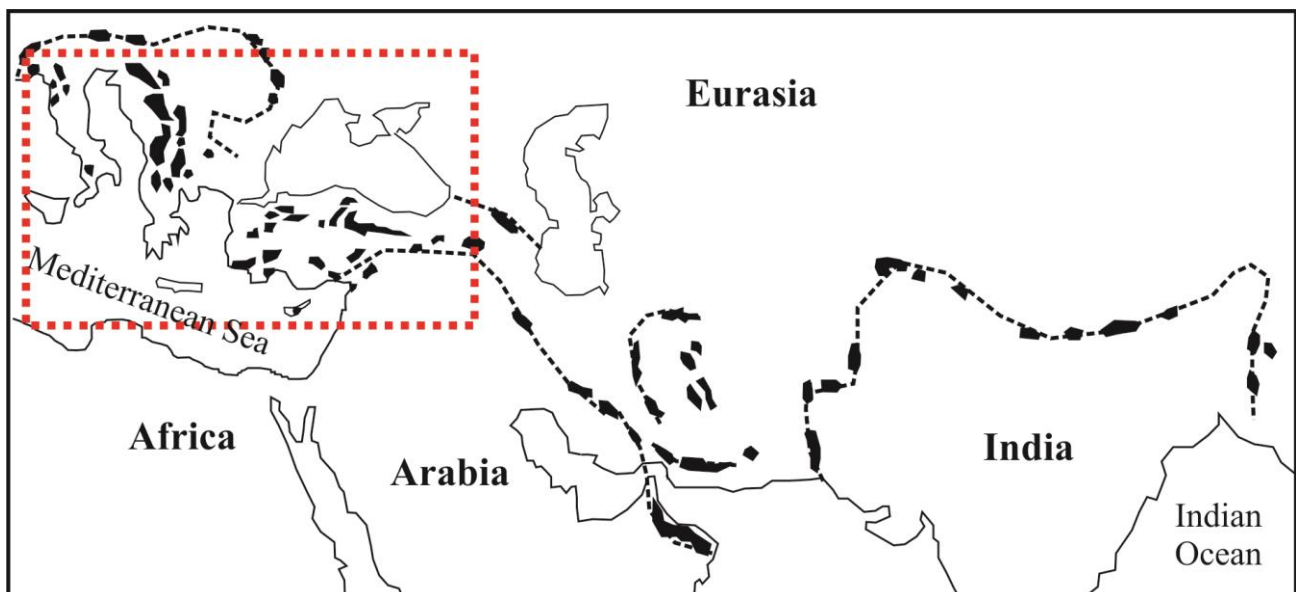


**Figure 1.** Distribution of major Tethyan ophiolites and suture zones in the Alpine-Himalayan orogenic system. Simplified after Dilek et al. [5]. The red dashed line box indicates the overviewed area.

There is a general consensus that podiform chromitites originate from the interaction between compositionally variable melts and upper mantle rocks [9–11]. Podiform chromitites are categorized based on their chemical composition into high-Cr (metallurgic type with  $\text{Cr}_2\text{O}_3$  contents between 45 and 60 wt% and  $\text{Cr}\# > 0.6$ ) and high-Al (refractory type with  $\text{Al}_2\text{O}_3 > 25$  wt% and  $\text{Cr}\# < 0.6$ ) types [10]. The distribution of high-Cr and high-Al chromitites is primarily controlled by different geotectonic settings (subduction-related or unrelated) and stratigraphic positions relative to the mantle–crust transition zone (MTZ). The mineral chemistry of chromitites reflects the melt composition from which they crystallized, with high-Cr and high-Al chromitites related to boninitic and mid-ocean ridge basalt (MORB) magmas, respectively [9].

In the Mediterranean Basin, podiform chromitites from the northern Italian Apennines, the Balkans, Turkey, and Cyprus occur mainly in the mantle section and, to a lesser extent, in the MTZ and some cumulus sequences of Tethyan ophiolites. This contribution presents an overview based on approximately 2000 electron microprobe analyses of chromite grains and 596 whole-rock analyses of PGE from chromitites associated with Tethyan ophiolites of the Mediterranean Basin. We discuss the possible relationships between chromite composition and PGE distribution in these chromitites to better understand factors such as the degree of partial melting of the mantle source, PGE fractionation during parent melt crystallization, and the prevailing geodynamic setting during chromitite precipitation in ophiolites.

## 2. Geological Background and Chromitite Description of Tethyan Ophiolites in the Mediterranean Basin

Ophiolites comprise sections of oceanic crust and underlying upper mantle that have been uplifted and emplaced in orogenic belts, such as the Alpine-Himalayan belt (Figure 1), one of the largest in the world [5]. The complete stratigraphy of an ophiolite, from base to top, includes variably serpentinized mantle peridotites and a crustal sequence composed of (1) cumulate mafic–ultramafic rocks, (2) a sheeted dike complex with multiple vertical, parallel dikes, (3) basaltic pillow lavas, and (4) sediments, mainly limestone and chert [14]. Tethyan ophiolites in the Mediterranean region (Figure 1) represent fragments of the lithosphere that floored the western wing of the Tethys Ocean during the Cretaceous and Jurassic periods [6–8,15]. They are mainly distributed in Italy, the Balkan Peninsula, the Aegean Islands, Turkey, and Cyprus (Figure 2A–D). The vast Tethyan orogenic belt comprises several segments forming subparallel tectonic sutures, named according to their geographic location, such as the Ligurian ophiolites or Ligurides of Italy [16].

Ophiolite complexes in the Balkan Peninsula form NNW-SSE trending belts known as the Dinarides (Croatia, Bosnia, Serbia, Kosovo), the Albanides (Albania), and the Hellenides (North Macedonia, Bulgaria, and Greece) [17]. Ophiolites in Turkey extend roughly in a W-E direction and are divided into three major belts [18]: (1) the Pontides, extending from Izmir–Bursa–Eskisehir (NW Turkey) to the Sivas–Erzincan–Kopdag–Erzurum zone (NE Turkey); (2) the Anatolides, between the Tuz Gölü and Pinarbasi zone (central Turkey); and (3) the Taurides, extending from Mugla–Antalya, the Pozanti–Karsanti and Mersin zones (S Turkey) to Hatay–Kahramanmaraş (SE Turkey), Elazığ, and Van Gölü zones (E Turkey) [6–8]. The Tauric belt includes the Troodos ophiolite complex of Cyprus. Dating of the metamorphic soles of ophiolites [19] indicates Upper Jurassic ages for the Dinarides, Albanides, and Hellenides and predominantly Cretaceous ages for the Pontides, Anatolides, and Taurides. Regional geology suggests that ophiolites in these provinces formed in several adjacent basins separated by microcontinents rather than fragments of a single, large ocean [6]. Several studies [6–8,20] show that most Tethyan ophiolites in the eastern Mediterranean basin formed in an SSZ, whereas only a few generated at a MOR tectonic regime [21].

Most of the chromitite reserves in Europe are hosted in ophiolite complexes in the Balkans, Turkey, and Cyprus [22–33], with smaller deposits in the northern Apennines of Italy [21]. The chromite composition and PGE distribution of the reviewed chromitites have been published in several papers (Table 1). These chromitites occur in the following ophio-

lite complexes, listed from west to east by host country: (1) Italy: Bracco [21] (Figure 2A), (2) Serbia: Veluce [34] (Figure 2B), (3) Albania: Mirdita–Bulqiza [35–38] (Figure 2B), (4) Greece: Pindos [32,34,39–44], Vourinos [34,39,45–49], Othrys [32,39,50,51], Edessa [34], Thessaly [32,34,39,52], Euboea (Evia) [34], Skyros [34,45,53], western Chalkidiki [25,32,34,54–56], eastern Chalkidiki [25,34,54,57,58], Rhodope Massif [34] (Figure 2B), (5) Kosovo: Brezovica [34], Ljuboten–Radusa [34] (Figure 2B), (6) Turkey: Antalya–Isparta [59], Berit [60,61], Doğanşehir [61], Guleman [62,63], Islahiye–Gaziantep [64], Kahramanmaraş [65], Pozanti–Karsanti [66], Elmaslar [67], Köyceğiz [68], Muğla–Ortaca [69–72], Bursa–Harmancık [73], Bursa–Orhaneli [73], Elekdag [74], Eskişehir [75], Kop [76], Tunceli [77] (Figure 2C), and (7) Cyprus: Troodos [78–80] (Figure 2D).

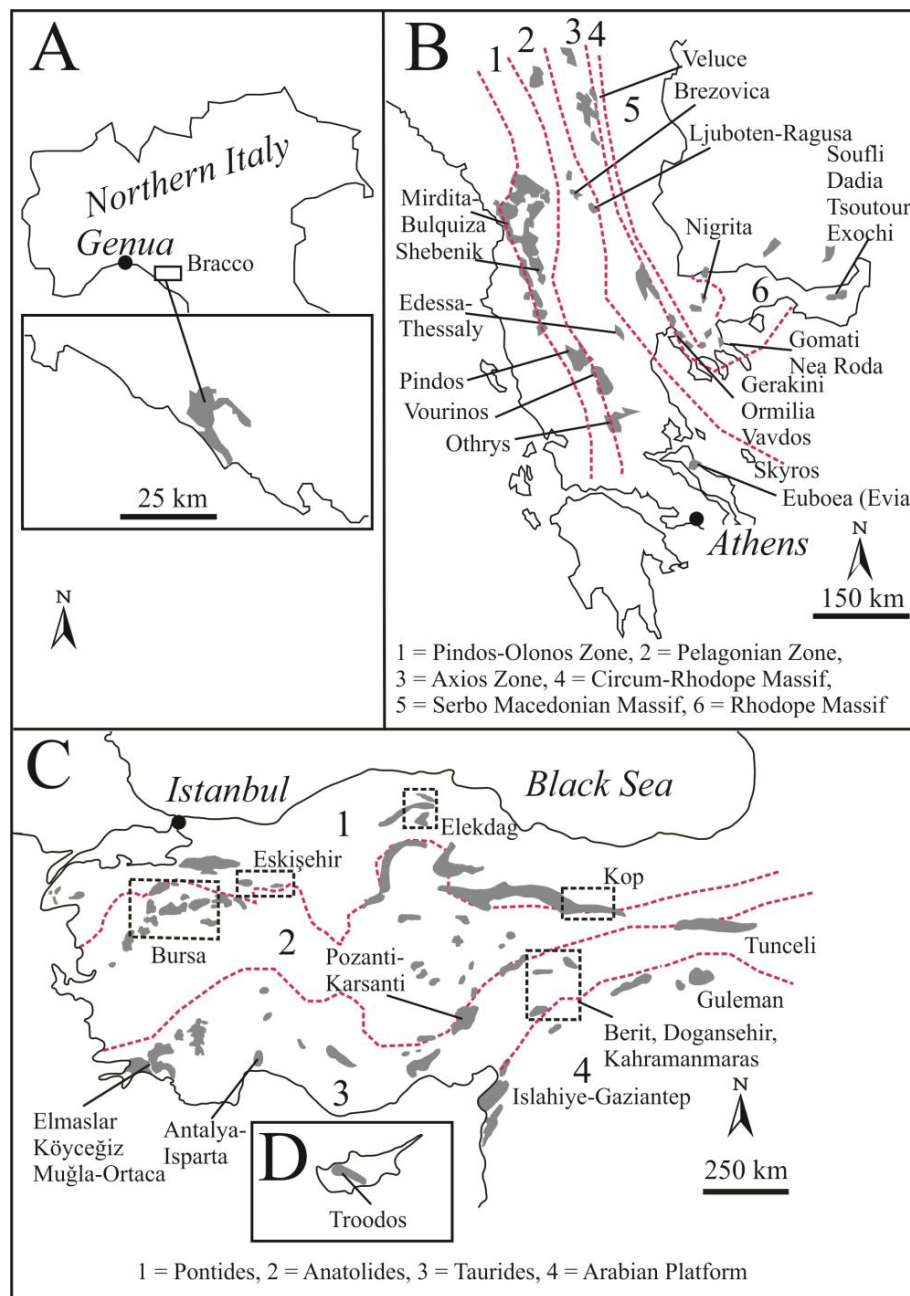


**Figure 2.** Location of ophiolites hosting the overviewed chromitites. (A) Ligurian ophiolite of Italy, (B) ophiolites of the Balkan Peninsula, (C) ophiolites of Turkey, and (D) ophiolite of Cyprus. The tectonic zones of Figures (B,C) are taken from Jacobshagen et al. [17] and Ketin [18].

**Table 1.** Ophiolitic chromitites from the Mediterranean Basin overviewed in this contribution listed from west to east according to their host country.

Country	Ophiolite	Tectonic Unit	Name of the Deposit	Stratigraphy	Host Peridotite	Chromite Type	References
ITALY	Bracco	Internal Ligurides	Canegreca, Cima Stronzi, Mattarana, Pian della Madonna, Ziona	Mantle–cumulate	Lherzolite	High-Al	[21]
SERBIA	Veluce	Axios Zone	Veluce	Mantle	Lherzolite–harzburgite–dunite	High-Cr	[34]
ALBANIA	Mirdita–Bulqiza	Pindos–Olonos Zone	Bulqiza Bulqiza-Ceruja Bulqiza-Bater Bulqiza-Qaf Dardhe	Mantle–MTZ Mantle–MTZ Mantle MTZ	Harzburgite	High-Cr High-Al High-Cr High-Al	[35–37]
	Shebenik	Pindos–Olonos Zone		Mantle–MTZ	Harzburgite	High-Cr	[38]
GREECE	Pindos	Pindos–Olonos Zone	Dramala Kambos Despoti Kyra Kali Korydallos-Gournes Milia Trygona Vourbiani	Mantle Mantle Mantle Mantle–MTZ–cumulate Mantle Mantle Mantle	Harzburgite–dunite	High-Cr High-Cr High-Cr High-Al, High-Cr High-Cr High-Cr High-Al	[32,39–44]
	Vourinos	Western side of the Pelagonian Zone	Aetoraches Doumarachi Kissavos Kondro Keratsista Koursumia Mikroklisoura Pefka Rizo Rodiani-Zygosti Tsouka Voidolakkos Xerolivado	Mantle Mantle Mantle–MTZ Mantle Mantle Mantle Mantle–MTZ Mantle Mantle Mantle Mantle Mantle Mantle	Harzburgite–dunite	High-Cr High-Cr High-Al, High-Cr High-Cr High-Cr High-Cr High-Cr High-Cr High-Cr High-Al High-Cr High-Cr High-Cr	[34,39,45–49]

Table 1. Cont.

Country	Ophiolite	Tectonic Unit	Name of the Deposit	Stratigraphy	Host Peridotite	Chromite Type	References
GREECE	Othrys	Pelagonian Zone	Agio Stefanos	Mantle	Lherzolite	High-Al	[32,39,50,51]
			Domokos	Mantle		High-Al	
			Eretria-Tsangli	Mantle		High-Al	
	Edessa	Pelagonian Zone	Edessa	Mantle	Harzburgite	High-Cr	[34]
	Thessaly	Pelagonian Zone	Fitia Giannakochori Mavrolivado Veria (Galaktos) Vermion	Mantle	Harzburgite–lherzolite	High-Cr High-Cr High-Cr High-Cr High-Cr	[25,32,34,52]
				Mantle			
				Mantle			
				Mantle			
	Euboea (Evia)	Pelagonian Zone	Madoudi Nea Artaki	Mantle Mantle	Harzburgite	High-Al, High-Cr High-Cr	[34]
	Skyros	Pelagonian Zone	Achladoses Agios Iannis	Mantle	Harzburgite	High-Al High-Cr	[32,34,45,53]
Mantle							
Western Chalkidiki	Circum-Rhodope Belt	Gerakini Ormilia Vavdos	Mantle Mantle Mantle	Harzburgite–dunite	High-Cr High-Cr High-Cr	[25,32,34,54–56]	
Eastern Chalkidiki	Serbo Macedonian Massif	Gomati (Paivouni, Tripes Agios Georgios, Kroupnos, Limonadika) Nigrita Nea Roda	Mantle	Harzburgite	High-Al, High-Cr	[25,34,54,57,58]	
			Mantle				
Rhodope Massif	Rhodope Massif	Dadia Exochi Soufli Tsoutoura	Mantle Mantle Mantle Mantle	Harzburgite–dunite	High-Cr High-Cr High-Cr High-Al	[34]	
KOSOVO	Brezovica	Pelagonian Zone		Mantle	Harzburgite–dunite	High-Cr	[34]
	Ljuboten–Radusa	Pelagonian Zone		Mantle	Harzburgite	High-Cr	[34]

Table 1. Cont.

Country	Ophiolite	Tectonic Unit	Name of the Deposit	Stratigraphy	Host Peridotite	Chromite Type	References
TURKEY	Elmaslar	Western Taurides, Lycian Nappe		Mantle	Harzburgite	High-Cr	[67]
	Köyceğiz	Western Taurides, Lycian Nappe		Mantle	Harzburgite	High-Cr	[68]
	Muğla–Ortaca	Western Taurides, Lycian Nappe	Catal, Sandalbasi, Bulusblu, Zeytinli, Payamli	Mantle	Harzburgite–dunite	High-Al, High-Cr	[69–72]
	Antalya–Isparta	Central–Western Taurides, Antalya Suture Zone		Mantle	Harzburgite	High-Al, High-Cr	[59]
	Pozanti–Karsanti	Eastern Taurides	Kızılyüksek	Mantle–MTZ–cumulate	Harzburgite	High-Cr	[66]
	Berit	Eastern Taurides	Palith Alish, Dereağzı, Kırcuşağı, Payamly, Sarıkat	Mantle MTZ–cumulate	Harzburgite	High-Al, High-Cr	[60,61]
	Doğanşehir	Eastern Taurides		Mantle	Harzburgite	High-Al, High-Cr	[61]
	Kahramanmaraş	Eastern Taurides	Adiyaman, Elbistan, Heikimhan, Kara, Malatya Turkoglu	Mantle	Harzburgite	High-Al, High-Cr	[65]
	Tunceli	Eastern Taurides, Izmir–Ankara–Erzincan Suture Zone	Yıldırım, Aksu, Hasangazi, Atilla, Eskigedik, Işıkvuran, Oymadal	Mantle	Harzburgite	High-Cr	[77]
	Eskişehir	Pontides, Izmir–Ankara–Erzincan Suture Zone	Dağköplü, Kavak	Mantle	Harzburgite	High-Cr	[75]
	Elekdağ	Pontides, Sakarya Zone		Mantle	Harzburgite–dunite	High-Al, High-Cr	[74]
	Kop	Pontides, Erzincan–Erzurum	Bal, Çalışkan, Engin, Ezan, G. Bülent, Gözeler, Gürel, Irem, K. Bülent, Kurtaran, Okutan, Selin, Sulu	MTZ	Harzburgite	High-Cr	[76]

Table 1. Cont.

Country	Ophiolite	Tectonic Unit	Name of the Deposit	Stratigraphy	Host Peridotite	Chromite Type	References
TURKEY	Bursa–Harmancık	Anatolides, Izmir–Ankara–Erzincan Suture Zone		Mantle	Dunite	High-Cr	[73]
	Bursa–Orhaneli	Anatolides, Izmir–Ankara–Erzincan Suture Zone		Mantle	Dunite	High-Cr	[73]
	Guleman	Arabian Platform, Elazig Zone	Bati Kef, Alacakaya	Mantle	Harzburgite–dunite	High-Cr	[62,63]
	Islahiye–Gaziantep	Arabian Platform, Bitlis–Zagros Suture Zone		Mantle	Harzburgite–dunite	High-Cr	[64]
CYPRUS	Troodos	Taurides	Hadji Pavlou Kannoures Kokkinorotsos	Mantle Cumulate Cumulate Mantle Mantle Mantle	Harzburgite Harzburgite–dunite Harzburgite–dunite Harzburgite	High-Cr High-Cr High-Cr High-Cr High-Cr High-Cr	[78–80]



### 2.1. The Chromitites of Italy and Their Host Ophiolites

The Ligurian ophiolites in the north Italian Apennines are remnants of the oceanic crust that floored the Piedmont–Ligurian Tethys during the Jurassic period [81] and are divided into two main units: the External Ligurides and the Internal Ligurides, corresponding to different lithostratigraphic and tectonic settings [82]. These units represent the oceanic formations and their peri-continental margins, with the External Ligurides being more distal within the oceanic basin. They are characterized by an anomalous stratigraphy that deviates from the ideal ophiolite sequence. Notably, the sheeted dike complex and cumulate rocks are absent. Instead, a lherzolitic mantle with a sub-continental petrologic signature is intruded by several layered gabbros, while pillow lavas and pelagic sediments lie directly on the mantle tectonite [16]. Thick horizons of ophicalcite and ophiolitic breccias, generated by seafloor erosion of plutonic and volcanic rocks, are common in the Ligurian ophiolites.

According to the classification proposed by Dilek and Furnes [8], the Ligurian ophiolites are considered subduction-unrelated, continental-margin types. These characteristics distinguish the ophiolites of northern Italy from those in the eastern Mediterranean, which mainly formed in a subduction geodynamic environment [6,20]. The only data available for Italy pertain to the chromitites found in the Bracco ophiolite complex of the Internal Ligurides [21] (Figure 2A and Table 1). The Bracco chromitites occur in a gabbroic body that intrudes mantle lherzolite. They form small rhythmic layers of Al-rich chromitite that resemble the stratiform chromitites found in large continental layered intrusions. Due to their small size, they have only been prospected but have never been mined. Chromite compositions and PGE contents of chromitites from Canegreca, Cima Stronzi, Mattarana, Pian della Madonna, and Ziona [21] are reviewed in this paper (Table 1).

### 2.2. The Chromitites of Albania and Their Host Ophiolites

Late Jurassic ophiolites occur in the Albanides, specifically in the Pindos–Olonos Zone (Table 1 and Figure 2B). These ophiolites are arranged in two subparallel belts: a western and an eastern one, each characterized by different petrologic and metallogenic features [22,24,83]. The ophiolites of the western belt consist predominantly of lherzolitic mantle overlain by cumulate sequences (dunite, troctolite, wehrlite, gabbro) and MORB-type volcanics. A true sheeted dike complex is absent. Based on petrologic and structural characteristics, these ophiolites are believed to have formed in a MOR setting [83]. Chromitites in the western belt are limited, and only a few data on their composition are provided by Cina et al. [22].

The ophiolites of the eastern belt demonstrate affinities similar to SSZ-type suites, with a few exceptions showing features transitional from MOR- to SSZ-type. They consist of large mantle tectonite formations with predominant harzburgite–dunite lithology, overlain by ultramafic–mafic cumulates (dunite, lherzolite, wehrlite, gabbro) and a thin sheeted dike complex. The different geodynamic settings and diachronous mantle evolution in the Albanides are supported by the variable geochemical signatures and ages of volcanic rocks. These include (1) Triassic transitional to alkaline within-plate basalts (WPB), (2) Triassic normal (N-MORB) and enriched MORB (E-MORB), (3) Jurassic N-MORB, (4) Jurassic basalts with a composition intermediate between MORB and island arc tholeiites (IAT), and (5) Jurassic boninites [84].

The most important chromitite deposits in Albania occur in harzburgite mantle tectonites located in the SSZ ophiolites of the eastern belt. These chromitite deposits extend from north–northwest to southeast, associated with the Tropojia–Kukes–Kalimashi, Mirdita–Bulqiza, and Shebenik ophiolite complexes. They include massive pods and schlieren-type deposits occurring at four stratigraphic levels in the ophiolite sequences [22]. Levels 1 and 2 are found at the lower and upper parts of the mantle unit in the ophiolite massifs of Tropojia, Kukes, Bulqiza, and Shebenik. Level 3 and 4 chromitites are associated with ultramafic cumulates in the mantle–crust transition zone of the Bulqiza complex and in the supra-Moho layered sequence of the Tropojia suite. Chromium reserves in the Bulqiza and Tropoja massifs sum up to about 25 Mt [24]. Despite the abundant deposits, PGE data,

coupled with chromite composition for the Albanian chromitites, are limited to the deposits of the Bulqiza and Shebenik ophiolites [22,35–38] (Figure 2B and Table 1).

### 2.3. The Chromitites of Serbia and Kosovo and Their Host Ophiolites

The Late Triassic to Jurassic, MOR-type ophiolite complexes of Serbia and Kosovo are dominated by lherzolitic and lherzolitic–harzburgitic mantle, similar to the western Albanides [24,29]. These complexes contain subeconomic deposits of high-Al chromitites [29]. Small lherzolite–harzburgite–dunite complexes in central Serbia represent transitional MOR–SSZ types within the Axios Zone [85] (Figure 2B). These mantle units contain small chromitite deposits (e.g., Veluce) with high-Cr chromite, although estimated reserves of chromium do not exceed a few thousand tons [34].

The most important deposits of high-Cr chromitite occur in the SSZ-type Ljuboten–Raduša and Brezovica ophiolite blocks, which belong to the Pelagonian Zone in Kosovo (Figure 2B), near the borders with Albania and North Macedonia. At Ljuboten–Raduša, several individual bodies of massive chromitite, up to 1.2 Mt, are distributed along the foot- and hanging-wall contacts of a 3.5 km thick body of harzburgite and dunite. The middle zone of the ophiolite predominantly consists of harzburgite and contains schlieren-type chromite mineralization [28,29]. In the Brezovica ophiolite complex, several mines have been described [29,30,32,34], but few PGE data coupled with chromite composition are available for chromitites from Veluce (Serbia) and Raduša (Kosovo) [32,34] (Figure 2B and Table 1).

### 2.4. The Chromitites of Greece and Their Host Ophiolites

The Albanides and Dinarides extend southward through North Macedonia into northern and central Greece. In this region, the Hellenides are subdivided into several subparallel tectonic regions: the Pindos–Olonos Zone, the Pelagonian Zone, the Axios Zone, the Circum-Rhodope Belt, and the Serbo-Macedonian and the Rhodope Massifs (Figure 2B and Table 1). These zones contain ophiolite complexes that are remnants of a sub-oceanic lithosphere of the western limb of Mesozoic Tethys [86]. Recent reinterpretations of their petrological and metallogenic characteristics suggest diverse geodynamic origins, including subduction-related and non-subduction-related environments, such as axial rifting zones [6,34,55,87]. Some Greek ophiolites host chromite deposits of varying size and economic importance [34].

#### 2.4.1. The Pindos–Olonos Zone Chromitites

The Pindos ophiolite complex, situated in the Pindos–Olonos Zone (Figure 2B), exhibits transitional characteristics from MOR- to SSZ-type. It comprises a large harzburgite–lherzolite mantle tectonite and a broad range of volcanic rocks from MORB to IAT and boninite-type [6,88]. The Pindos complex hosts only a few small chromitite deposits characterized by massive, schlieren, and nodular textures, irregularly distributed in the mantle harzburgite (<0.1 Mt total) [34,41,89]. Chromitites are also found in the MTZ and supra-Moho cumulates. PGE distribution and chromite composition data are available for chromitite deposits such as Dramala, Kambos Despoti, Kyra Kali, Milia, Trygona, Vourbani, and the Korydallos–Gournes chromitites occurring in the MTZ of the Pindos ophiolite [32,34,39–44] (Table 1).

#### 2.4.2. The Pelagonian Zone Chromitites

Several ophiolites in the Pelagonian Zone of the Hellenides host chromitite deposits that were historically mined. These include Vourinos, Othrys, Edessa, Thessaly, Euboea (Evia), and Skyros (Figure 2B and Table 1).

The Vourinos complex, on the western side of the Pelagonian Zone (Figure 2B), is an SSZ-type ophiolite emplaced on lower Jurassic sediments and unconformably overlain by Cenomanian limestone. It primarily consists of harzburgite–dunite mantle tectonite with subordinate mafic–ultramafic cumulates, overlain by IAT and boninite-type vol-

canic rocks [6,26,34,90]. More than 700 occurrences of chromitite ores, including some of Greece's largest mines, have been documented in the Vourinos ophiolite, which contains the country's largest chromite deposits totaling about 10 Mt of ore. Chromitites are typically found in mantle tectonites, displaying massive, pod, schlieren, and minor nodular textures. Prominent investigations into PGE distribution and chromite mineral chemistry have focused on deposits such as Aetoraches, Doumarachi, Kissavos, Kondro Keratsista, Koursumia, Mikroklistoura, Pefka, Rizo, Rodiani-Zygosti, Tsouka, Voidolakkos, and Xerolivado [34,39,45–49,91] (Table 1).

The Othrys ophiolite complex in eastern central Greece (Figure 2B) comprises serpentinized upper mantle harzburgite and lherzolite with minor dunite, overlain by gabbroic cumulates and mafic dikes. Similar to Pindos, the Othrys complex features volcanic rocks with geochemical affinities ranging from MORB to IAT and boninite [92]. Metallogenic data [34,51] indicate that the Othrys ophiolite developed within a complex geotectonic system transitioning from an oceanic spreading center to an SSZ regime. Major chromite deposits are found within two tectonically separated ultramafic bodies: Metalion, Aghio Stefanos, and Domokos in the Domokos area and Eretria, Mavro, Tsagli, and Kastraki in Eretria. Podiform and massive chromitites, totaling over 3 Mt, have been historically mined in both Domokos and Eretria blocks. Due to poor outcrops and significant tectonic alteration, the precise stratigraphic position of Othrys chromitites within the mantle section remains challenging to establish. PGE data and chromite composition information are available from the Aghio Stefanos, Domokos, and Eretria-Tsangli mines [32,39,50,51] (Table 1).

Several small, subeconomic chromite deposits are found in mantle peridotites, mainly harzburgite, of ophiolites in Edessa, Thessaly, and the Aegean islands of Skyros and Euboea (Evia) (Figure 2B). Despite their limited size and economic significance, investigations into their PGE distribution and chromite mineral chemistry have been conducted [32,34,52,53] (Table 1).

#### 2.4.3. The Circum-Rhodope Belt, Serbo-Macedonian, and Rhodope Massif Chromitites

The Chalkidiki Peninsula in northern Greece is a geologically complex area where the Circum-Rhodope Belt and the Serbo-Macedonian Massif juxtapose in tectonic contact, whereas the latter overthrusts the Rhodope Massif to the east (Figure 2B). The Circum-Rhodope Belt consists of low-grade metamorphic Triassic and Jurassic sedimentary rocks, while the Serbo-Macedonian and the Rhodope Massifs comprise high-grade metamorphic rocks [93]. The Circum-Rhodope Belt outcrops in western Chalkidiki and contains fragments of strongly serpentinized and tectonized ophiolitic ultramafic rocks. These ultramafic rocks are predominantly harzburgite–dunite mantle tectonites hosting approximately 50 small-sized chromitites, which have never been mined. The chromitites exhibit schlieren, massive, and nodular textures [26]. PGE contents and chromite composition data are available for chromitites associated with the Gerakini, Ormilina, and Vavdos ophiolites in western Chalkidiki [25,32,34,54–56] (Table 1).

The Serbo-Macedonian and Rhodope Massifs are exposed in Serbia, North Macedonia, Greece, and Bulgaria. They comprise rocks metamorphosed in the amphibolite-facies, forming the basement of the Alpine orogenic belt. The Serbo-Macedonian Massif in Greece, located in eastern Chalkidiki (Figure 2B), includes Paleozoic ophiolite blocks composed of serpentinized ultramafic rocks representing mantle tectonites [26]. Despite their low economic potential, several thousand tons of ore have been recovered in the past from a few small chromitite bodies in this area. These chromitites have been investigated for their PGE distribution and mineral chemistry by multiple authors [25,34,54,57,58] (Table 1). A segment of the metamorphic Rhodope Massif crops out in the Thrace region of Greece, east of the Serbo-Macedonian (Figure 2B) and south of the border with Bulgaria. In this area, ultramafic rocks comprising harzburgite–dunite represent a portion of the Paleozoic suboceanic mantle affected by polyphase regional metamorphism in an SSZ environment [94]. These rocks host small podiform chromitites that have undergone similar metamorphic

evolution as their hosts [34]. Limited PGE data and chromite compositions are available from the Dadia, Exochi, Soufli, and Tsoutoura chromitites of the Rhodope Massif [34] (Table 1 and Figure 2B).

### 2.5. The Chromitites of Turkey and Their Host Ophiolites

Chromite represents a crucial economic resource for Turkey, with over 2000 deposits of podiform chromitites documented to date. Consequently, Turkey ranks among the world's leading chromium producers [27,75]. Most Turkish chromitites are podiform and are located within the mantle sequences of ophiolite complexes, distributed from north to south in the Pontides, Anatolides, and Taurides, as well as to the east on the Arabian Platform [95,96] (Figure 2C). These mantle peridotites were emplaced during the Alpine orogeny from the Upper Jurassic to Cretaceous periods and predominantly consist of depleted dunite–harzburgite, which is partially to completely serpentinized. Petrologically and chemically, the Turkish ophiolites demonstrate petrological and geochemical affinities typical for subduction-related oceanic lithosphere [6]. Chromitites in Turkey are dispersed throughout the country, with a concentration in the southern regions associated with the Taurides Belt (Figure 2C), which harbors over 90% of Turkey's chromite reserves [27].

#### 2.5.1. The Taurides Belt Chromitites

The ophiolites associated with the Tauride orogenic belt of Turkey extend from the Lycian nappes in the west to the Divriği ophiolite in the east [97]. These ophiolites host numerous chromite deposits, totaling approximately 2000. However, only a few have been comprehensively analyzed for both PGE distribution and mineral chemistry. These include, from west to east, the Elmaslar, Köyceğiz and Muğla–Ortaca complexes in the western Taurides belt [67–72], Antalya–Isparta in the central–western Taurides near the Antalya Suture Zone [59], and the Pozanti–Karsanti, Berit, Doğanşehir, Kahramanmaraş, and Tunceli suites in the eastern Taurides Zone [60,61,64–66,77] (Figure 2C and Table 1). The Lycian nappe complex overlays the autochthonous Menderes Massif and Bey Dağ platform and consists, from base to top, of metasediments, a mélangé unit, and an ophiolitic sequence [68–71]. These ophiolites formed in an SSZ regime and comprise predominantly allochthonous blocks of mantle harzburgite with subordinate dunite and lherzolite, along with isolated gabbro–dolerite dikes. The depleted mantle tectonites of Elmaslar, Köyceğiz, and Muğla–Ortaca contain massive, schlieren, and occasionally nodular chromitites that have undergone detailed analysis for PGE content and chromite composition [67–81] (Table 1). Notable chromite mining sites in the Ortaca area include Catal, Sandalbasi, Bulusblu, Zeytinli, and Payamli [69]. Some occurrences in Muğla demonstrate MORB-type affinities, and the currently active Muğla–Ortaca ophiolite hosts several chromite deposits totaling approximately 2 Mt [69–71].

In the central–western Taurides, specifically the Antalya Suture Zone, the Antalya–Isparta ophiolite consists of SSZ-type rocks with small bodies of massive and schlieren chromitites (Figure 2C). This ophiolite represents remnants of the southern branch of Neotethyan oceanic basins and is predominantly composed of mantle peridotites, with harzburgite being the most abundant, accompanied by minor lherzolite and dunite. PGE distribution and chromite mineral chemistry data have been reported by [59] (Table 1).

The Pozanti–Karsanti ophiolite complex in the eastern Taurides Belt of southern Turkey contains chromite deposits totaling up to 1.98 Mt [27] (Figure 2C). It comprises mantle tectonites, ultramafic and mafic cumulates, isotropic gabbros, sheeted dikes, and volcanic rocks [98]. Chromitites are predominantly found in mantle dunites near the Moho transition zone and in cumulate dunites in the Kızılyüksek area [66]. Chromite textures include massive pods associated with mantle peridotites and banded formations in cumulate dunites. PGE and chromite composition analyses have focused on the Kızılyüksek chromitites [66] (Table 1).

The Berit, Doğanşehir, and Kahramanmaraş ophiolite complexes in the eastern Taurides Zone consist of metaophiolitic rocks intruded by calc-alkaline granitoid intrusions

(Figure 2C). These metaophiolites include metaharzburgite, metadunite, granulite, amphibolites, schist, metagabbro, and metavolcanic rocks [65]. Chromite deposits such as Palith, Alish, Dereağzı, Kırçıuşağı, Payamly, and Sarikat have been studied for PGE analyses and chromite composition [61,66] (Table 1). Most chromitites occur as small lenses associated with dunite pods within the MTZ, except for Palith, which forms small, massive pods surrounded by dunite envelopes in harzburgite [60]. Chromite textures range from massive to nodular, occasionally appearing as banded schlieren [61–65]. Numerous small chromite deposits, totaling up to 2 Mt, have been described at Kahramanmaraş [65].

In the eastern Taurides near the Izmir–Ankara–Erzincan Suture Zone, the Tunceli ophiolite hosts several chromite mines, including Yıldırım, Aksu, Hasangazi, Atilla, Eskigedik, Işıkvuran, and Oymadal, which have recently been subject to whole-rock PGE content and mineral chemistry studies [77] (Table 1). The Tunceli complex comprises a nearly complete ophiolite sequence of mantle peridotite, gabbros, sheeted dikes, pillow lavas, and sediments [77]. Mantle peridotite mainly consists of serpentinized harzburgite hosting podiform chromitites, predominantly observed in massive textures with subordinate nodular textures.

### 2.5.2. The Pontides Belt Chromitites

Several chromite deposits associated with the ophiolites of Eskişehir, Elekdağ, and Kop have been studied for their PGE contents and chromite compositions in the Pontides Belt (Figure 2C and Table 1) [74–76]. The Eskişehir ophiolite, located in the Izmir–Ankara–Erzincan Suture Zone near the Anatolides Belt (Figure 2C), is tectonically disrupted and heavily serpentinized. It comprises (1) a restitic mantle primarily composed of harzburgite with subordinate dunite, intersected by diabase dikes; (2) cumulate dunite, wehrlite, pyroxenite, and gabbros; (3) a sheeted dike complex; and (4) plagiogranite dikes cutting across the gabbro and sheeted dike complex [99]. Harzburgite is the dominant rock type in the Eskişehir ophiolite. Several podiform chromitites, locally mined, are typically enclosed within dunite. Among them, the chromite deposits of Dağküplü and Kavak have been studied by Uysal et al. [75].

In the Sakarya Zone of the central Pontides, small-scale chromite deposits with a maximum resource of several thousand tons are described in serpentinized harzburgite and dunite of the Elekdağ meta-ophiolite (Figure 1). The Elekdağ complex has undergone metamorphism from greenschist to mid-amphibolite facies, affecting the associated peridotite and chromitites. The Elekdağ chromitites have been studied for their PGE content and chromite composition by Donmez et al. [74] (Table 1).

The Kop ophiolite, situated in the Erzincan–Erzurum area of the Pontides Belt (Figure 2C), is interpreted as a forearc lithospheric fragment of the Neo-Tethys ocean. It comprises an incomplete ophiolite sequence, consisting of a harzburgitic upper mantle unit with rare lherzolite in contact with an MTZ predominantly composed of cumulate dunite. Pyroxenite dikes crosscut the harzburgite and dunite [76]. Massive and banded chromitites occur in the Kop ultramafic rocks and have been investigated for their PGE distribution and chromite mineral chemistry by Uysal et al. [76]. Data are available for Bal, Çalışkan, Engin, Ezan, G. Bülent, Gözeler, Gürel, Irem, Bülent, Kurtaran, Okutan, Selin, and Sulu deposits.

### 2.5.3. The Anatolides Belt Chromitites

Whole-rock PGE analyses and chromite compositions are provided for the chromitites associated with the Harmançık and Orhaneli complexes hosted in the Bursa ophiolite of the Anatolides belt by Uysal et al. [73] (Table 1 and Figure 2C). The Upper Cretaceous, incomplete Bursa ophiolite represents a remnant of the northern branch of the Neo-Tethyan Ocean. According to Sarifakioğlu et al. [100], the Harmançık complex comprises serpentinized mantle peridotites, while the Orhaneli complex represents the MTZ. The Orhaneli MTZ consists of a magmatic layering of ultramafic cumulates with minor gabbro, locally cut by diabase dikes [100]. Banded and lenticular bodies of massive chromitites, mainly associated with dunites, have been described in both the Harmançık and Orhaneli complexes [73].

#### 2.5.4. The Arabian Platform Chromitites

The chromitites associated with the ophiolites of Guleman [62,63] and Islahiye–Gaziantep [64], located in the Arabian Platform of Turkey, have been studied for their PGE distribution and chromite composition (Figure 2C and Table 1).

The Guleman ophiolite consists of harzburgite–dunite mantle tectonite, locally intruded by mafic dikes and emplaced in the Elazig zone of the Arabian Platform during the Upper Cretaceous [27]. This unit is overlain by a cumulate pile composed of dunite, pyroxenite, wehrlite, troctolite, and gabbro. Sheeted dikes and pillow lavas are absent [27]. The Guleman ophiolite hosts approximately 20 podiform chromite deposits associated with the mantle tectonite, totaling about 10.5 Mt (production + reserves). Two of these deposits, Bati Kef and Alacakaya, have been specifically investigated for their PGE distribution and chromite composition [62,63] (Table 1).

The Islahiye–Gaziantep podiform chromitites occur in the Bitlis–Zagros Suture Zone of the Arabian Platform (Figure 2C). In this area, the ophiolite consists solely of strongly serpentinized mantle peridotites. Despite the alteration, blocks of harzburgites and dunites have been identified. Small-sized pyroxenite dikes crosscut the mantle peridotite. The serpentinized peridotites are in tectonic contact with Upper Maastrichtian limestone, shale, and sandstones [64]. Chromite compositions and PGE abundances for the Islahiye–Gaziantep chromitite can be found in the study by Yapici et al. [64] (Table 1).

#### 2.6. The Chromitites of Cyprus and Their Host Ophiolite

The Late Cretaceous Troodos ophiolite complex occurs in the southernmost part of the central Tauride province of Cyprus (Figure 2D). It consists of a depleted harzburgitic mantle with subordinate dunite and lherzolite, overlain by a sequence of cumulus dunite, wehrlite, websterite, gabbro, and anorthosite. This sequence transitions upwards into a sheeted dike complex and pillow lavas. The volcanic rocks exhibit compositions strongly influenced by subduction, with characteristics transitioning from island arc tholeiite (IAT) to boninite-type, although mid-ocean ridge (MOR)-type basalts have also been reported [6,31]. Economic chromitite deposits in the Troodos ophiolite are primarily restricted to dunite lenses within the harzburgitic tectonite in the Mt. Olympus plutonic complex, totaling more than 1 Mt, although all mining activities are currently closed [31,101]. Additional chromitite bodies occur in the cumulus dunite and at the transition between cumulus dunite and cumulus wehrlite [79], though they do not reach the size of economically exploitable deposits. The Troodos ophiolite hosts chromitites both as podiform bodies within the mantle harzburgite and as smaller layers within the overlying dunites of the cumulate sequence. The podiform chromitite deposits of Hadji Pavlou, Kokkinorotsos, and Kannoures have been investigated for their chromite composition and PGE distribution [31,78–80]. Only two layered chromitites occurring in the cumulate sequence have been analyzed by McElduff and Stumpfl [79] (Table 1).

### 3. Distribution of High-Al and High-Cr Chromitites in Ophiolitic Complexes

The data summarized in Table 1 encompass 74 chromitite deposits hosted within 33 ophiolite complexes. Based on their Cr#, the majority of these chromitites are classified as high-Cr chromitites, with fewer categorized as high-Al chromitites. Some deposits exhibit the co-existence of both high-Al and high-Cr chromitites. Figure 3A illustrates that 68% of the surveyed deposits consist of high-Cr chromitites, 14% of high-Al chromitites, and 18% of both high-Al and high-Cr chromitites. The statistical distribution of these chromitite types, categorized by their host ophiolites, is depicted in Figure 3B. This figure shows that 49% of the surveyed ophiolites host exclusively high-Cr chromitites, 45% host both high-Al and high-Cr chromitites, and 6% host only high-Al chromitites.

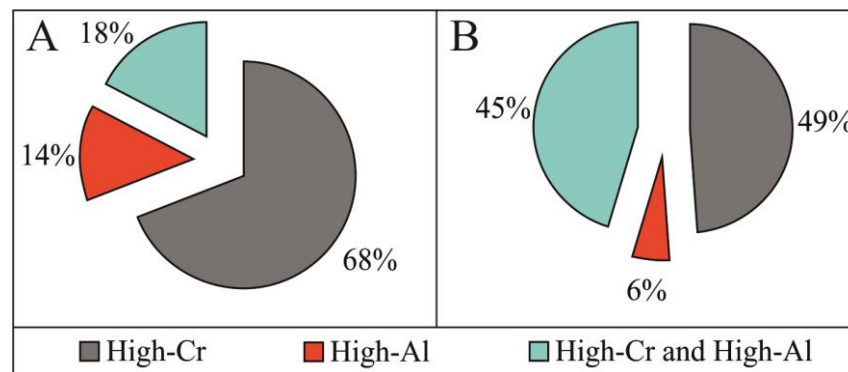


**Figure 3.** Statistical distribution of the high-Al and high-Cr chromitites of the Mediterranean Basin overviewed in this contribution. (A) Distribution according to their ophiolite host; (B) distribution based on the host single deposit.

High-Cr chromitites are reported exclusively in chromitites from the following ophiolites (Table 1): Veluce [34] (Serbia), Shebenik [38] (Albania), Edessa [34], Thessaly [32,34,39,52], western Chalkidiki [25,32,34,54–56] (Greece), Brezovica, Ljuboten–Radusa [34] (Kosovo), Elmaslar [67], Köyceğiz [68], Pozanti–Karsanti [66], Tunceli [77], Eskişehir [75], Kop [76], Bursa–Harmancık and Bursa–Orhaneli [73], Guleman [62,63], Islahiye–Gaziantep [64] (Turkey), and Troodos [78–80] (Cyprus).

These high-Cr chromitites are predominantly hosted in mantle tectonites composed of harzburgite with minor dunite. The Veluce chromitites are unique in occurring within a mantle peridotite consisting mainly of lherzolite, harzburgite, and dunite (Table 1). Few instances of high-Cr chromitites are documented in the MTZ and cumulates (Table 1).

The Bracco and Othrys ophiolites, located in Italy and Greece, respectively, exclusively host high-Al chromitites associated with lherzolite and harzburgite mantle peridotites [21,32,39,50,51] (Table 1). In the Bracco ophiolite, these chromitites occur as thin layers associated with gabbro intruding sub-continental mantle peridotite, present both in the mantle sequence and MTZ. Only a small number of high-Al chromitites have been identified within the cumulates of the Berit ophiolite in Turkey [60].

The co-existence of high-Al and high-Cr chromitites is observed in several ophiolites, including Mirdita–Bulqiza [35–37] (Albania), Pindos [32,34,39–44], Vourinos [34,45–49], Euboea (Evia) [34], Skyros [32,34,45,53], eastern Chalkidiki [25,34,54,57,58], Rhodope Massif [34] (Greece), Muğla–Ortaca [69–71], Antalya–Isparta [59], Berit [60,61], Doğanşehir [61], Kahramanmaraş [65], and Elekdağ [74] (Turkey). However, within individual ophiolite complexes, high-Cr chromitites generally outnumber their high-Al counterparts (Table 1).

#### 4. Distribution of PGE in Chromitites

A comprehensive analysis of 596 whole-rock PGE analyses from the reviewed chromitites is detailed in Supplementary Material Table S1. These analyses cover all six PGE, although some values are below detection limits. The distribution of PGE varies significantly, with total PGE contents ranging from a few parts per billion (ppb) to a remarkable 28,830 ppb (Supplementary Material Table S1).

Based on the PPGE/IPGE ratios, chromitites are categorized into two groups: (1) high-IPGE, with PPGE/IPGE ratios below 1, and (2) high-PPGE, with PPGE/IPGE ratios above 1. The PPGE/IPGE ratios exhibit considerable variability among the reviewed chromitites, ranging from 0.01 to an extraordinary 61.39, although the majority show ratios below 1 (Supplementary Material Table S1). Figure 4A illustrates that only 10% of the reviewed chromitites are classified as high-PPGE. Notably, within the Mediterranean Basin, 70% of these high-PPGE chromitites are categorized as high-Al, whereas 30% are high-Cr (Figure 4B). Chondrite-normalized [102] PGE spidergrams for chromitites from Italy, Albania, Serbia, Kosovo, and Greece are depicted in Figure 5A–N, while Figure 6A–O illustrate those from Turkey and Cyprus.

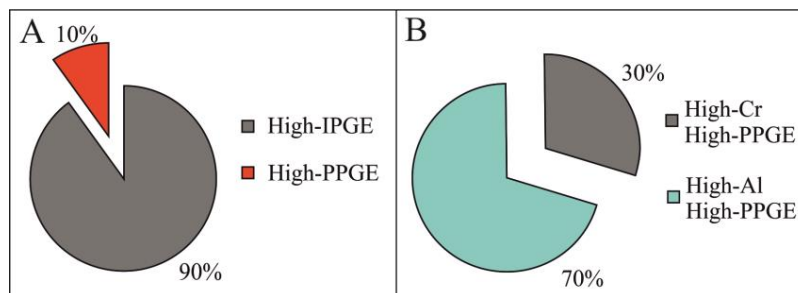


**Figure 4.** Statistical distribution of the overviewed high-IPGE and high-PPGE chromitites. (A) High-IPGE and high-PPGE frequencies of all the overviewed chromitites and the (B) frequency based on the chromite composition.

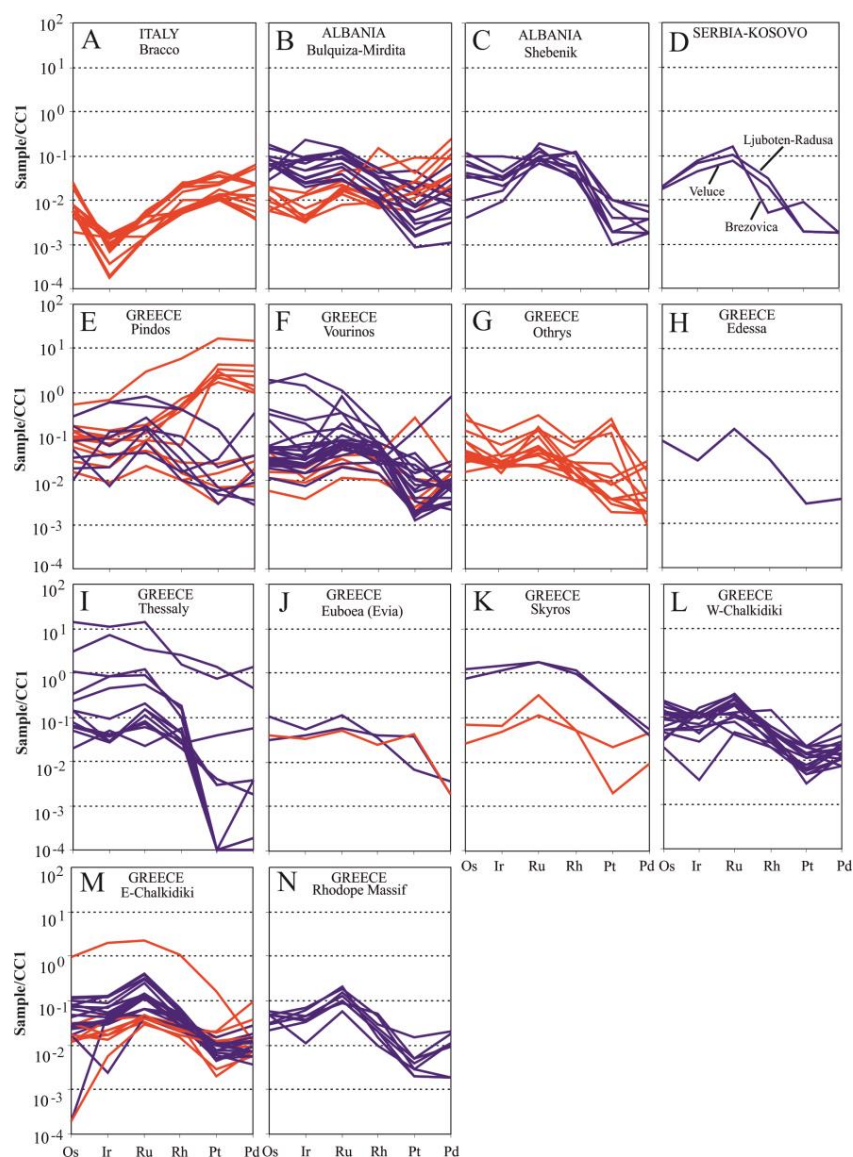


**Figure 5.** Chondrite-normalized [102] PGE patterns of the overviewed chromitites, according to the geographical location of the host ophiolites. (A) Bracco, Italy; (B) Bulqiza–Mirdita, Albania; (C) Shebenik, Albania; (D) Serbia and Kosovo; (E) Pindos, Greece; (F) Vourionos, Greece; (G) Othrys, Greece; (H) Edessa, Greece; (I) Thessaly, Greece; (J) Euboea (Evia), Greece; (K) Skyros, Greece; (L) W-Chalkidiki, Greece; (M) E-Chalkidiki, Greece; (N) Rhodope Massif, Greece. Red line = high-Al chromitite, blue line = high-Cr chromitite. See Table 2 for data source and references.



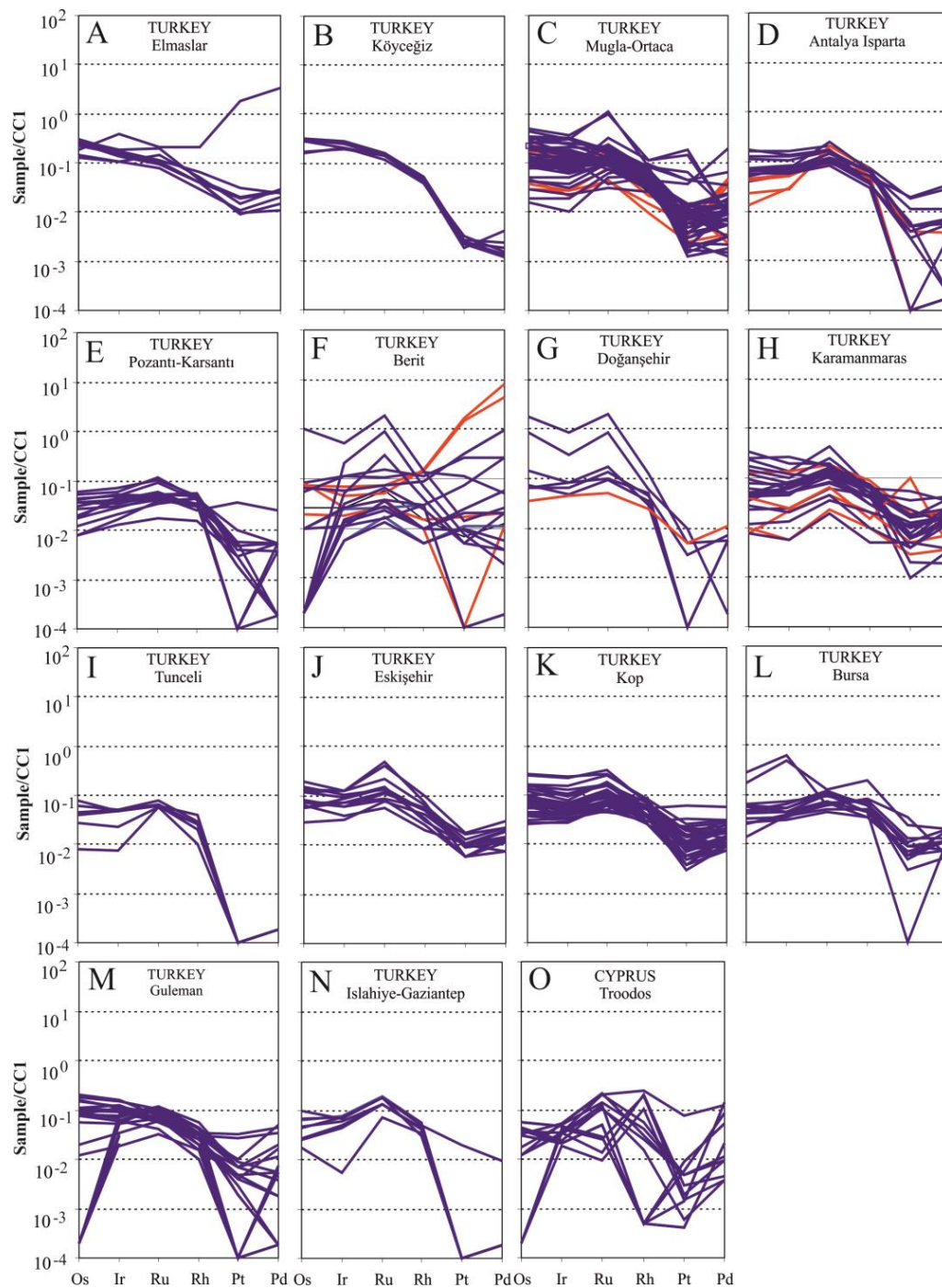


**Figure 6.** Chondrite-normalized [102] PGE patterns of the overviewed chromitites, according to the geographical location of the host ophiolites. (A) Elmaslar, Turkey; (B) Köyceğiz, Turkey; (C) Mugla–Ortaca, Turkey; (D) Antalya–Isparta, Turkey; (E) Pozanti–Karsanti, Turkey; (F) Berit, Turkey; (G) Doğanşehir, Turkey; (H) Karamanmaras, Turkey; (I) Tunceli, Turkey; (J) Eskişehir, Turkey; (K) Kop, Turkey; (L) Bursa, Turkey; (M) Guleman, Turkey; (N) Islahiye–Gaziantep, Turkey; (O) Troodos, Cyprus. Red line = high-Al chromitite, blue line = high-Cr chromitite. See Table 2 for data source and references.

**Table 2.** Whole-rock analyses (ppb) in the overviewed chromitites (-: below detection limit).

	Os	Ir	Ru	Rh	Pt	Pd	ΣPGE	Pd/Ir	Pt/Pt*	PPGE/IPGE
					High-Al					
Average	37	35	84	22	329	199	512	9.67	1.36	3.14
Minimum	-	-	1	1	-	1	17	-	0.01	0.02
Maximum	481	1080	2100	1140	17,100	7860	28,830	178.60	14.42	61.39
					High-Cr					
Average	77	81	138	15	59	26	396	1.03	0.64	0.66
Minimum	-	1	-	-	-	-	20	-	-	0.01
Maximum	7400	6020	9700	510	3460	1815	24,940	150.91	39.21	62.6

$$Pt/Pt^* = (Pt/8.3)/\sqrt{[(Rh/1.6) \times (Pd/4.4)]}, [103].$$

#### 4.1. PGE Distribution in the Chromitites of Italy

A comprehensive analysis of 16 whole-rock PGE data sets has been conducted for the high-Al chromitites associated with the Bracco ophiolite [21]. These chromitites exhibit low ΣPGE contents ranging from 12 to 68 ppb, with an average of 44 ppb. Chondrite-normalized [102] PGE spidergrams depicted in Figure 5A illustrate a negative Ir anomaly and a steep positive slope overall, indicating an enrichment of PPGE over IPGE. The PPGE/IPGE ratio ranges from 3.05 to 10.89. The PGE patterns of the Bracco chromitites resemble typical stratiform chromitites, differing from the negative PGE slope typically seen in mantle-hosted podiform chromitites.

#### 4.2. PGE Distribution in the Chromitites of Albania

In Albania, 33 PGE analyses cover both high-Al and high-Cr chromitites hosted in the mantle and MTZ of the Bulquiza–Mirdita ophiolite [25–37], with additional data available for high-Cr chromitites in the mantle sequence of the Shebenik ophiolite [38]. The total PGE contents vary widely, ranging from 70 to 280 ppb in high-Cr chromitites (average 163 ppb) and 38 to 228 ppb in high-Al chromitites (average 99 ppb).

Chondrite-normalized PGE spidergrams from Bulquiza–Mirdita show a pronounced negative slope between IPGE and PPGE in high-Cr chromitites, contrasting with less fractionated patterns in high-Al chromitites (Figure 5B). The PPGE/IPGE ratio ranges from 0.05 to 0.41 in high-Cr chromitites and 1.04 to 4.28 in high-Al chromitites. Nine whole-rock PGE published analyses of chromitites from the Shebenik ophiolite derive only from high-Cr types, which are hosted in the mantle and MTZ [38]. The total PGE amounts range between 79 and 197 ppb, with PPGE/IPGE ratios ranging from 0.05 to 0.41. The chondrite-normalized PGE spidergrams closely resemble those of the high-Cr chromitites of Bulquiza–Mirdita (Figure 5B,C).

#### 4.3. PGE Distribution in the Chromitites of Serbia and Kosovo

Three bulk-rock PGE analyses are available for the mantle-hosted high-Cr chromitites of the Veluce (Serbia), Brezovica, and Ljuboten–Radusa (Kosovo) ophiolites, reporting low ΣPGE contents: 92 ppb in Veluce, 170 ppb in Brezovica, and 125 ppb in Ljuboten–Radusa [34]. All these chromitites exhibit similar PGE spidergrams (Figure 5D), characterized by a notable negative slope between IPGE and PPGE. The Brezovica chromitites also display variable negative and positive anomalies for Rh and Pt.

#### 4.4. PGE Distribution in the Chromitites of Greece

A substantial number of Greek ophiolitic chromitites have been analyzed for their PGE contents, with a total of 191 published by several authors (Table 1). Mantle-hosted chromitites in the Pindos ophiolite generally show enrichments in PGE, although noble metals are unevenly distributed among the analyzed samples (Figure 5E) [33,34,40–44]. Total PGE abundances in high-Al ores range from 43 ppb up to 28,830 ppb (average 3135 ppb) and 94 ppb up to 3871 ppb (average 840) in high-Cr deposits.

The highest PGE values were detected in a sample collected from the Korydallos mine, occurring in the MTZ and the cumulates, where abundant alloys considered remnants of base metal sulfides occur as inclusions in chromite crystals and as interstitial phases in the silicate matrix [44]. PPGE/IPGE ratios range between 0.54 and 62.6 in high-Al chromitites and between 0.07 to 24.64 in high-Cr chromitites. Chondrite-normalized PGE patterns of high-Cr chromitites typically display a negative slope between IPGE and PPGE, with some samples enriched in Pd (Figure 5E). High-Al chromitites exhibit highly variable PGE patterns, ranging from nearly flat to positive (Figure 5E).

A notable difference in PGE distribution is observed between high-Al and high-Cr chromitites in the Vourinos ophiolite (Figure 5F) [34,39,45–49]. Total PGE amounts in high-Al deposits are low, ranging between 27 ppb and 348 ppb (average 116 ppb), with PPGE/IPGE ratios between 0.32 and 5.44. High-Cr chromitites are enriched in  $\Sigma$ PGE, with contents varying from 29 ppb to 3030 ppb (average 297 ppb) and PPGE/IPGE ratios ranging from 0.02 to 16.77. Chondrite-normalized PGE patterns of high-Cr chromitites typically show a negative slope from IPGE to PPGE, with occasional enrichments in Pd and a weak positive anomaly of Pt observed in one sample (Figure 5F). PGE patterns of high-Al chromitites are similar to those of high-Cr chromitites but generally less fractionated and with lower total amounts (Figure 5F), with only one chromitite displaying a notable Pt-positive anomaly (Figure 5F).

High-Al chromitites hosted in the mantle lherzolite of the Othrys ophiolite contain total PGE amounts ranging from 53 ppb to 540 ppb (average 151 ppb), with the highest PGE content observed in the sulphide-rich chromitites of the Eretria complex [32,39,50,51]. PPGE/IPGE ratios range from very low values of 0.05 up to 5.72 in the sulphide-rich chromitite of Eretria. Chondrite-normalized PGE patterns of high-Al chromitites in the Domokos complex of the Othrys ophiolite resemble those of high-Cr chromitites, showing a negative slope from IPGE to PPGE and a positive peak of Ru. The sulphide-rich chromitites of the Eretria complex also exhibit pronounced Pt- and Pd-positive and -negative anomalies, respectively (Figure 5G).

The ophiolites of Edessa and Thessaly in the Pelagonian Zone contain only mantle-hosted high-Cr chromitites analyzed for their whole-rock PGE contents [33,34,39,52,67–81]. Only one analysis has been provided for the Edessa chromitite, showing low PGE values of 166 ppb and a PPGE/IPGE ratio of 0.07. More data are available for Thessaly chromitites, which exhibit significant variation in PGE distribution, ranging from 62 ppb to 24,940 ppb. Extremely high PGE values have been reported in chromitites of Veria (Galaktos), which are generally PGE-rich [52]. PPGE/IPGE ratios range between 0.01 and 0.65. Chondrite-normalized PGE patterns of both Edessa and Thessaly chromitites (Figure 5H,I) exhibit negative slopes, with enrichments in IPGE relative to PPGE.

High-Al and high-Cr chromitites in the mantle tectonite of Euboea (Evia) ophiolite exhibit very similar PGE contents and spidergrams, showing an enrichment in IPGE, although two samples exhibit a positive peak of Pt (Figure 5J). Total PGE concentrations in analyzed chromitites are low, ranging from 123 ppb to 176 ppb (average 142) [32]. PPGE/IPGE ratios in Euboea (Evia) chromitites vary from 0.1 to 0.68.

PGE contents in chromitites from the mantle harzburgite of the Skyros ophiolite range between 321 and 354 ppb (average 338 ppb) in high-Al chromitites and between 136 and 3078 ppb (average 2075 ppb) in high-Cr chromitites [32,34,45,53]. PPGE/IPGE ratios in Skyros chromitites range between 0.1 and 0.68. Despite significant variations in total PGE contents, high-Al and high-Cr chromitites of Skyros display negatively sloped chondrite-normalized PGE patterns, although with differences in Pt and Pd ratios resulting in positive and negative slopes in high-Al and high-Cr chromitites, respectively (Figure 5K).

Mantle-hosted high-Cr chromitites associated with the western Chalkidiki ophiolite show total PGE values ranging from 71 to 431 ppb (average 257 ppb) [25,32,34,54,56], with PPGE/IPGE ratios ranging from 0.07 to 0.65. Chondrite-normalized PGE patterns of western Chalkidiki chromitites align well with other mantle-hosted ophiolitic chromitites, characterized by negative slopes from IPGE to PPGE (Figure 5L). A few samples exhibit

a marked negative peak of Ir, and only one sample is enriched in Rh (Figure 5L). Total PGE abundance in eastern Chalkidiki chromitites, hosted in a mantle tectonite, ranges between 45 and 3516 ppb (average 467 ppb) in high-Al chromitites and between 64 and 419 ppb (average 191 ppb) in high-Cr chromitites [25,34,54,57,58]. PPGE/IPGE ratios range between 0.13 and 1.32 in high-Al chromitites and between 0.05 and 0.64 in high-Cr chromitites. Both high-Al and high-Cr chromitites exhibit similar PGE profiles and generally display negatively sloped chondrite-normalized PGE patterns with positive Ru anomalies. However, the chromitite collected from the Tripes mine exhibits higher PGE enrichment except for Pd (Figure 5M) [57], with a few chromitites exhibiting negative peaks of Os and Ir (Figure 5M).

High-Cr chromitites analyzed in the mantle peridotite of the Rhodope Massif exhibit total PGE contents ranging from 42 ppb to 198 ppb (average 142) [34], with PPGE/IPGE ratios ranging between 0.03 and 0.35. According to PGE spidergrams (Figure 5N), Rhodope chromitites closely resemble typical mantle-hosted ophiolitic chromitites, being enriched in IPGE relative to PPGE.

#### 4.5. PGE Distribution in the Chromitites of Turkey

With 332 published bulk-rock analyses, Turkish chromitites are extensively studied in the Mediterranean Basin for their PGE distribution.

The Elmaslar ophiolite, in the western Taurides, contains high-Cr chromitites within its mantle section, exhibiting varying PGE contents, ranging from 217 to 428 ppb (average 315 ppb) and PPGE/IPGE ratios 0.08–0.18 [67]. Their chondrite-normalized patterns generally show IPGE predominance over PPGE, typical for ophiolitic podiform chromitites (Figure 6A). Exceptionally, one sulfide-enriched chromitite contains anomalously high contents of  $\Sigma$ PGE = 4145 ppb (predominantly due to high Pt and Pd concentrations up to 1830 ppb and 1815 ppb, respectively) and shows a high PPGE/IPGE ratio of 8.05 (Figure 6A).

The Köyceğiz ophiolite, within the western Taurides, contains high-Cr massive chromitites in the mantle harzburgite and displays variable PGE distributions (277–441 ppb, average 336 ppb) and consistent PPGE/IPGE ratios (0.03–0.04). Chondrite-normalized patterns exhibit negative slopes from Os to Rh, with steep gradients between Rh and Pd and occasional positive slopes between Pt and Pd (Figure 6B) [68].

The Muğla–Ortaca ophiolite in the western Taurides hosts both high-Al and high-Cr chromitites in its mantle tectonites, studied for their PGE contents [69–72]. High-Al and high-Cr chromitites exhibit similar chondrite-normalized PGE patterns, although high-Al samples generally have slightly lower total PGE amounts, ranging from 73 to 367 ppb (average 201 ppb), compared to 63 to 1305 ppb (average 283 ppb) in high-Cr chromitites. All chromitites show higher IPGE contents than PPGE, with PPGE/IPGE ratios ranging from 0.08 to 0.73 in high-Al chromitites and 0.04 to 1.43 in high-Cr chromitites. Most samples display a Ru-positive peak relative to Ir and Rh, and some exhibit relatively high Pt and Pd contents (Figure 6C).

In the mantle harzburgite of the Antalya–Isparta ophiolite in the central–western Taurides, total PGE abundances vary between 148 and 164 ppb (average 153 ppb) in high-Al chromitites and between 125 and 366 ppb (average 197 ppb) in high-Cr chromitites [59]. PPGE/IPGE ratios range from 0.06 to 0.43 in high-Al chromitites and 0.07 to 0.16 in high-Cr chromitites. Both high-Al and high-Cr chromitites are characterized by an enrichment in IPGE relative to PPGE, resulting in negatively sloping chondrite-normalized PGE patterns (Figure 6D).

The Pozanti–Karsanti high-Cr chromitites in the eastern Taurides, hosted in mantle harzburgite near the MTZ, contain low total PGE amounts ranging from 32 to 162 ppb (average 91) [66]. PPGE/IPGE ratios vary from 0.11 to 0.75, and chondrite-normalized PGE diagrams show nearly flat to positive slopes from Os to Rh and negative slopes from Rh to Pt and Pd. All chromitites exhibit marked positive Ru anomalies (Figure 6E).

Chromitites from the Berit ophiolite in the eastern Taurides show a wide variability in PGE distribution, resulting in distinct chondrite-normalized PGE patterns (Figure 6F). Total PGE contents range widely, from 70 to 7301 ppb (average 2117 ppb) in high-Al and 41 to 2140 ppb (average 384 ppb) in high-Cr chromitites. Both types display negative and positive PGE patterns; some high-Al chromitite samples exhibit nearly flat patterns. Most high-Cr chromitites show pronounced Ru anomalies, although Os is often below the detection limit. PPGE/IPGE ratios range from 0.10 to 61.39 in high-Al and 0.03 to 10.18 in high-Cr chromitites (Figure 6F).

The Doğanşehir ophiolite, eastern Taurides, hosts high-Al and high-Cr chromitites in its mantle section, analyzed by Akmaz et al. [61]. Total PGE contents in high-Cr chromitites vary from 140 to 2774 ppb (average 781 ppb), whereas only one high-Al sample analyzed had  $\Sigma$ PGE = 94 ppb. PPGE/IPGE ratios are 0.21 in high-Al and range from 0.04 to 0.1 in high-Cr chromitites. All analyzed chromitites are enriched in IPGE relative to PPGE, with a positive Ru anomaly. High-Al chromitites generally show lower enrichment compared to other types, with Pd slightly higher than Pt in most samples (Figure 6G).

High-Al chromitites hosted in mantle harzburgite of the Kahramanmaraş ophiolite, eastern Taurides, contain PGE abundances ranging between 31 and 318 ppb (average 148 ppb). In the same complex, high-Cr chromitites co-exist with a total PGE of 71–441 ppb (average 214 ppb) [65]. PPGE/IPGE ratios range from 0.18 to 1.33 in high-Al and 0.03 to 0.68 in high-Cr chromitites. Both types exhibit negatively sloped chondrite-normalized PGE patterns with positive Ru anomalies. However, one high-Al sample shows a notable Pt-positive anomaly (Figure 6H).

The Tunceli ophiolite, eastern Taurides, contains only high-Cr chromitites in its mantle section, with  $\Sigma$ PGE values ranging from 52 to 114 ppb (average 92 ppb) [77]. PPGE/IPGE ratios range from 0.03 to 0.11, and chondrite-normalized PGE patterns are characterized by negative slopes with IPGE enrichment relative to PPGE (Figure 6I).

High-Cr chromitites from the Eskişehir ophiolite in the Pontides, hosted in mantle harzburgite, have total PGE amounts between 109 and 533 ppb (average 240 ppb) [75]. PPGE/IPGE ratios range from 0.08 to 0.3, resulting in negatively sloping chondrite-normalized PGE patterns. These patterns typically display a flat trend from Os to Ir, a positive Ru anomaly, a negative slope from Ru to Pt, and a weak positive trend from Pt to Pd (Figure 6J).

The Kop ophiolite in the Pontides hosts high-Cr chromitites in the MTZ, analyzed for their PGE distribution [76]. Total PGE contents range from 87 to 520 ppb (average 199 ppb), with PPGE/IPGE ratios from 0.12 to 0.68. Chondrite-normalized patterns show IPGE enrichment relative to PPGE, resulting in a negative slope from Os to Ru. Some samples exhibit a weak Pd enrichment over Pt (Figure 6K).

High-Cr chromitites from the complexes of Harmancık and Orhaneli in the Bursa ophiolite (Anatolides) show total PGE abundances between 83 and 574 ppb (average 188 ppb) in mantle-hosted high-Cr chromitites [73]. PPGE/IPGE ratios range from 0.14 to 0.51, and patterns are generally negatively sloped with a weak Ru-positive anomaly (Figure 6L). Some samples exhibit pronounced negative slopes with a positive Ir anomaly (Figure 6L).

The Guleman ophiolite in the Arabian Platform, analyzed by Page et al. [62] (however, no Os data provided) and more recently by Uysal et al. [63], includes high-Cr chromitites with low total PGE amounts ranging from 44 to 255 ppb (average 167 ppb). PPGE/IPGE ratios vary from 0.02 to 0.4, and chondrite-normalized PGE patterns typically show negative slopes from IPGE to PPGE (Figure 6M). Some samples exhibit positive slopes in the Pt to Pd segments.

Chromitites from the mantle section of the İslahiye–Gaziantep ophiolite in the Arabian Platform, analyzed for their PGE distribution by Yapıcı et al. [64], show low PGE amounts ranging from 67 to 235 ppb (average 169 ppb), and several analyses are too low and below detection limits. PPGE/IPGE ratios range from 0.03 to 0.18, and patterns exhibit

negatively sloped chondrite-normalized PGE patterns with IPGE predominance over PPGE (Figure 6N). A positive Ru anomaly is observed across all samples.

#### 4.6. PGE Distribution in the Chromitites of Cyprus

Despite their economic importance for chromium recovery in the past, the chromitites of the Troodos ophiolite in Cyprus have been poorly studied for their PGE distribution. Only 17 whole-rock analyses of the noble metals have been published so far [78–80]. Specifically, only high-Cr chromitites have been studied in the mantle sections of the Hadji Pavlou and Kokkinorotsos mines, as well as in the cumulates of the Kannoures and Kokkinorotsos mines. The available data indicate that the total PGE contents of the Troodos chromitites are low, ranging from 77 to 372 ppb (average 116 ppb), with the highest value detected in a single sample collected from the cumulate section [79]. The PPGE/IPGE ratio ranges between 0.05 and 1.65, resulting in variable chondrite-normalized PGE patterns (Figure 6O). The analyzed samples are characterized by negative chondrite-normalized PGE patterns with IPGE enrichments over PPGE [79,80], which is typical for mantle-hosted ophiolitic chromitites. Exceptionally, the PGE-rich sample from the cumulate section [79] displays a positive slope from Os to Ru and a relatively flat chondrite-normalized PGE pattern from Ru to Pd. In most of the analyses provided by Prichard and Lord [78], Os is very low or below detection limit, and Rh defines a marked positive anomaly relative to Ru and Pt (Figure 6O).

### 5. Comparative Analysis of PGE Content in High-Al and High-Cr Chromitites

Whole-rock PGE data from 109 high-Al and 487 high-Cr chromitites are reviewed in this paper. The average, minimum, and maximum values of the published PGE data highlight distinct differences between them (Table 2). High-Cr chromitites exhibit higher average values of Os (77 ppb), Ir (81 ppb), and Ru (138 ppb) compared to high-Al chromitites (37 ppb for Os, 35 ppb for Ir, and 84 ppb for Ru). Conversely, high-Al chromitites show higher average values of PPGE: 329 ppb for Pt and 199 ppb for Pd, compared to 59 ppb for Pt and 26 ppb for Pd in high-Cr chromitites. This results in differing PPGE/IPGE ratios between high-Al (average 3.14) and high-Cr (average 0.66) chromitites. High-Al chromitites also display a higher total PGE content, up to 512 ppb, compared to 396 ppb in high-Cr chromitites (Table 2).

Chondrite-normalized PGE patterns illustrate these differences: high-Al chromitites exhibit negative Ir anomalies and varied PGE patterns with occasional Pt-positive anomalies (Figure 7A). In contrast, high-Cr chromitites typically show IPGE enrichment, consistent with mantle-hosted ophiolitic chromitites, with some samples displaying Ru-positive anomalies and occasional PPGE enrichment (Figure 7B). Figure 7C portrays the average PGE values, highlighting similar IPGE behavior but differing distributions of Os, Ir, Ru, Pt, and Pd between high-Al and high-Cr chromitites. High-Al chromitites show, on average, as slightly negative, whereas high-Cr chromitites display flat Os-Ir patterns. High-Al chromitites show a pronounced positive slope from Rh to Pt, while high-Cr chromitites display a negative slope in this segment (Figure 7C).

Additionally, the Pt/Pt\* or Pt anomaly =  $(Pt_N / ((Rh_N \times Pd_N)^{0.5}))$  versus Pd/Ir diagram distinguishes residual mantle rocks from crystal-fractionation products [103], with most of the overviewed chromitites following a mantle restite melting trend (Figure 8A). This diagram by Leblanc [104] indicates that PGE contents increase with decreasing Pd/Ir ratios; hence, the high PGE amounts are related to Ir enrichments relative to Pd. The reviewed chromitites plot mainly in the IPGE-rich ophiolitic chromitites field, consistent with typical mantle-hosted deposits. A few exceptions include high-Al and rare high-Cr chromitites that plot in the PPGE-rich ophiolitic chromitites field (Figure 8B).

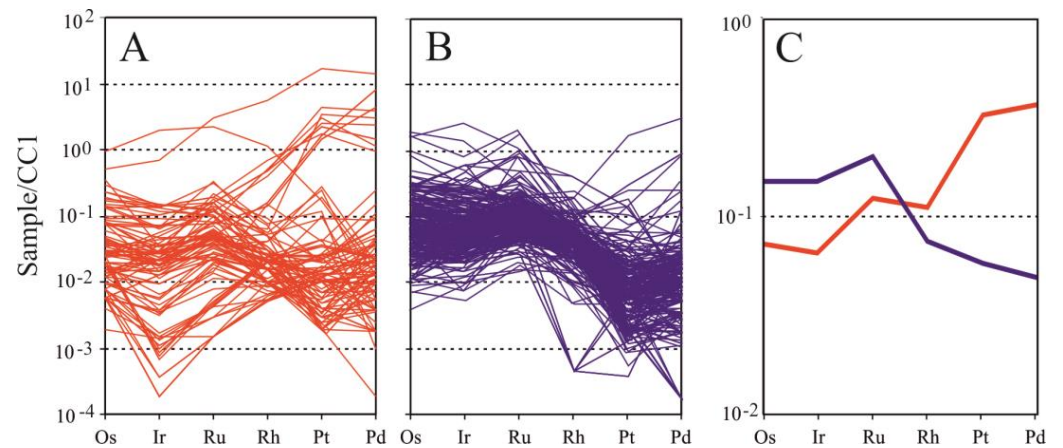


**Figure 7.** Chondrite-normalized [102] patterns of the overviewed chromitites with PGE values above detection limit, according to their chromite composition. (A) High-Al chromitites; (B) high-Cr chromitites; (C) average values of the high-Al and high-Cr chromitites. Red line = high-Al chromitite, blue line = high-Cr chromitite. See Table 2 for data source and references.

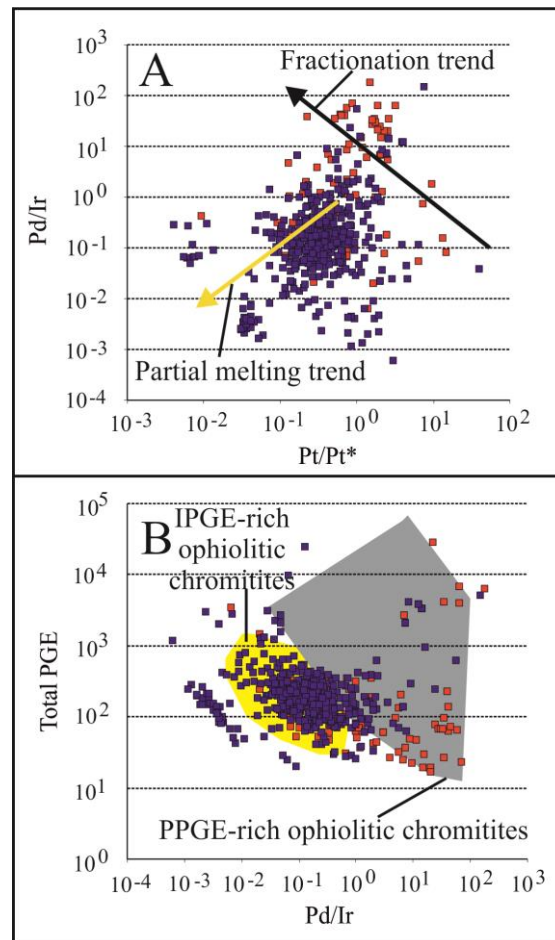


**Figure 8.** Binary diagrams for the overviewed ophiolitic chromitites. (A) Plot of the ratio Pd/Ir versus Pt/Pt\*, calculated after Garuti et al. [103]; (B) PGE contents versus Pd/Ir ratio and comparison with the IPGE-rich ophiolitic chromitite, redrawn after Leblanc [105]. IPGE-rich (yellow) and PPGE-rich (gray) fields after Zaccarini et al. [13].

## 6. Discussion

### 6.1. Significance of the Distribution of the High-Al and High-Cr Chromitites

For many decades, chromite composition has been considered a reliable petrogenetic indicator. High-Al chromitites are believed to form through the reaction of the fertile mantle with aluminous melts during ocean opening, such as at mid-ocean ridges or back-arc basins in supra-subduction zones [9]. High-Cr chromitites, on the other hand, are linked to SSZ environments, where depleted mantle interacts with high-Mg boninitic melts [9]. Johan et al. [104] proposed the significance of fluid-based processes in forming podiform chromitites. While supporting the widely accepted model of chromitite formation through melt–peridotite interaction, they suggested that large volumes of peridotite can be processed in an open, fluid-dominant reducing system through passive metasomatic processes. Fluid inclusions in chromite ore bodies indicate shallow marine hydrothermal systems, suggesting that heated seawater could play a role in chromitite formation [105].

Two major models explain the co-existence of high-Al and high-Cr chromitites in the same ophiolite. One model involves significant tectonic movements, leading to the formation of separate magma intrusions from differently depleted mantle sources, such as MORB versus boninite, with high-Al and high-Cr chromitites forming in different geodynamic settings during the regression of the oceanic lithosphere from the MOR towards SSZ [71]. The second model suggests that both high-Al and high-Cr chromitites were generated in an SSZ regime during the differentiation of a single batch of magma with initial boninitic composition, reacting with country rock peridotites. This results in a bimodal distribution and vertical zoning, with high-Cr chromitites in the deep mantle and Al-rich types at shallower levels close to the MTZ [105].

Boudier and Al-Rajhi [106] observed that lherzolite-type ophiolites (LOT), characterized by low degrees of mantle melting, rarely host significant chromite deposits. Conversely, numerous and larger chromite deposits occur in harzburgite-type ophiolites (HOT), representing products of high degrees of melting of a depleted mantle [107].

The chromitites in the Mediterranean Basin reviewed in this study align with these models. Most of the reviewed ophiolites (49%) exclusively host high-Cr chromitites (Figure 3B), which are associated with depleted mantle peridotites such as harzburgite and, rarely, dunite, forming large deposits. These ophiolites formed in SSZ environments following convergent plate tectonics, emphasizing the importance of this geodynamic setting in forming significant Cr deposits. Only two ophiolites, Bracco (Italy) and Othrys (Greece), exclusively host high-Al chromitites, representing 6% of all the reviewed ophiolites (Figure 3B). These deposits, hosted in fertile lherzolite (Bracco) and harzburgite (Othrys), are rare examples of high-Al chromitites formed in a distensive MOR environment in the Mediterranean Basin [21].

The model of high-Al chromitites precipitating at higher stratigraphic levels compared to high-Cr chromitites, due to differentiation of a boninitic melt reacting with the host mantle tectonite, applies to the Greek ophiolites of Pindos, Vourinos, and eastern Chalkidiki and Turkish chromitites in the Berit and Elekdağ ophiolites [60,74]. This model also fits the chromitites in the Greek ophiolites of Euboea, Skyros, and Rhodope despite tectonism and serpentinization complicating precise geological information.

The co-existence of high-Al and high-Cr chromitites has been reported in 45% of the reviewed ophiolites (Figure 3B). Cina et al. [22] observed that their distribution in Albania is mainly controlled by host peridotites (LOT versus HOT). In the Mirdita–Bulqiza ophiolite, high-Cr chromitites occur in the mantle, and high-Al ones in the MTZ [35–37].

A change in geodynamic settings from divergent to convergent is suggested to explain the bimodal distribution of high-Al and high-Cr chromitites in the Muğla–Ortaca, Doğanşehir, and Kahramanmaraş ophiolites of Turkey [61,65,69–72]. In the Muğla–Ortaca ophiolite, high-Al chromitites formed in an MOR environment through segregation of a melt from low-degree partial melting of a slightly depleted mantle. Co-existing high-Cr chromitites formed in an SSZ after ocean closure and subduction, with fluids from subducted crust increasing partial melting and forming boninitic magma [69–72].



In the Doğanşehir and Kahramanmaraş ophiolites, both high-Cr and high-Al chromitites formed in an SSZ setting. High-Cr chromitites crystallized from boninite melt, while high-Al chromitites precipitated in equilibrium with a MORB-type melt, likely in a back-arc basin [61,65].

#### 6.2. The Relation between the Chromite Composition and the PGE Distribution

Besides their economic importance, PGE, like chromite mineral chemistry, play a significant role in geological sciences. Their distribution helps establish (1) the degree of partial melting the mantle source underwent and (2) the crystal fractionation process, including the possible segregation of an immiscible sulfide liquid. High degrees of partial melting, up to 30%, are needed to remove all PGE, including the most refractory IPGE, from their mantle source, where they may occur as alloys and sulfides [108–110]. Lower melting degrees, between 20% and 25%, dissolve only preexisting sulfides, partially liberating PGE, especially the less refractory PPGE, into the melts [108].

Ophiolites formed in different oceanic geodynamic settings exhibit varying degrees of partial melting, from lower at MOR to higher degrees in SSZ, where significant mantle-crust interactions occur [109]. Although incipient to partial serpentinization may mobilize Pd and, to a lesser extent, Pt, it is generally agreed that this alteration process remobilizes PGE only on a small scale without significantly changing whole-rock PGE budget [110]. Thus, PGE provide valuable information about the petrological nature and evolution of the mantle source from which they and their host chromitites were derived.

Most ophiolitic high-Cr chromitites, including those of the Mediterranean Basin reviewed here, are preferentially enriched in refractory IPGE over PPGE, with an average PPGE/IPGE ratio of 0.66 (Figure 4A,B, Table 2). This results in well-defined PGE-negative slope patterns, with IPGE prevailing over PPGE (Figures 5, 6 and 7B,C). This enrichment is due to the compatible geochemical behavior of IPGE during the partial melting of the host mantle [110].

Most IPGE-rich chromitites in the Mediterranean Basin are hosted in highly depleted peridotites (Table 1) that interacted with boninitic melts, undergoing partial melting up to 30%, extracting refractory IPGE from their mantle source. Their restitic nature is reflected in most high-Cr chromitites plotting in the partial melting trend field in the Pd/Ir versus Pt/Pt\* diagram (Figure 8A).

High-Al chromitites in the Mediterranean Basin generally have a higher PPGE/IPGE ratio, up to 3.14, compared to high-Cr chromitites (Table 2). Their chondrite-normalized PGE patterns are more unfractionated (Figures 5, 6 and 7A), showing local enrichments in Pt and Pd (Figure 7C). These differences are observed in all reviewed high-Al chromitites, regardless of their occurrence in the mantle, MTZ, or supra-Moho cumulates (Table 1). The relatively low IPGE distribution and higher PPGE enrichment in high-Al chromitites hosted in the mantle can be attributed to the lower partial melting degree of their mantle source and crystallization from a MOR-type melt, which is poorer in IPGE than boninitic melts. High-Al chromitites formed at higher stratigraphic levels are believed to derive from a common and progressively evolving parental magma. Their PPGE enrichment can be attributed to a crystal fractionation process, consuming IPGE during the early precipitation of co-existing high-Cr chromitites in the deep mantle. Therefore, several high-Al chromitites align with a fractionation trend in the Pd/Ir versus Pt/Pt\* diagram (Figure 8A).

In line with Zaccarini et al. [13], most reviewed chromitites are enriched in IPGE, with only a few enriched in PPGE (Figure 4A,B). PPGE-enriched ores are mainly associated with high-Al chromitites (Figure 4B). According to PGE spidergrams, high-Al chromitites in Bracco (Figure 5A), Bulqiza–Mirdita (Figure 5B), Pindos (Figure 5E), and Berit (Figure 6F) and some high-Cr chromitites from Elmaslar (Figure 6A) and Berit (Figure 6F) show marked chondrite-normalized PGE positive patterns. The main mechanisms for PPGE enrichment in both high-Al and high-Cr chromitites include local sulfur saturation and the possible formation of an immiscible sulfide liquid collecting PPGE still available in the ore-forming system [13,23,60,67].

PPGE enrichment in the Bracco high-Al chromitite resulted from low partial melting of their mantle source, insufficient to remove all PGE, especially refractory IPGE [21]. Considering Pd mobilization by hydrothermal fluids, local Pd enrichment causing a weak positive trend in the Pt-Pd segment in several reviewed chromitites may be due to serpentinization affecting the host ophiolites.

## 7. Summary and Conclusions

Most chromitites in the Tethyan ophiolites of the Mediterranean Basin are classified as high-Cr and are enriched in refractory IPGE over PPGE, with an average PPGE/IPGE ratio of 0.66. These high-Cr chromitites formed in a SSZ environment, where the depleted mantle underwent up to 30% partial melting and interacted with high-Mg boninitic melts.

Less abundant high-Al chromitites have higher PPGE/IPGE ratios, up to 3.14, and relatively unfractionated PGE patterns with weak enrichments in Pt and Pd. They formed in an extensional regime and are associated with more fertile peridotites that experienced lower degrees of melting (20%–25%) and reacted with MORB melts.

The co-existence of high-Al and high-Cr chromitites in the same ophiolite can be explained by tectonic movements and separate intrusions of magmas from differently depleted mantle sources, such as MORB versus boninite. High-Al and high-Cr chromitites precipitated in different geodynamic settings during the regression of the oceanic lithosphere from MOR to SSZ.

Alternatively, both high-Al and high-Cr chromitites may have crystallized in a SSZ environment during the differentiation of boninitic magma reacting with country rock peridotites, resulting in a bimodal distribution and vertical zoning. High-Cr chromitites were deposited in the deep mantle, while Al-rich types formed higher in the stratigraphy, close to the MTZ.

Only a few reviewed ophiolitic chromitites display high-Al contents and PPGE enrichments due to local sulfur saturation and the possible formation of an immiscible sulfide liquid, which collected available chalcophile PPGE in the system.

**Supplementary Materials:** The following supporting information can be downloaded at: <https://www.mdpi.com/article/10.3390/min14080744/s1>, Table S1: PGE data of the overviewed chromitites.

**Author Contributions:** Conceptualization and data curation, F.Z., M.E.-E., B.T., and G.G.; Bibliographic research, F.Z., M.E.-E., B.T., and G.G.; Writing—original draft preparation, F.Z.; Writing—review and editing, F.Z., M.E.-E., B.T., and G.G. All authors have read and agreed to the published version of the manuscript.

**Funding:** This research did not receive external funding.

**Data Availability Statement:** Not applicable.

**Acknowledgments:** The authors would like to acknowledge the Editorial staff of Minerals and the three anonymous reviewers for their constructive comments, which helped to significantly improve the manuscript.

**Conflicts of Interest:** The authors declare no conflicts of interest.

## References

1. Arai, S. Genetic Link between Podiform Chromitites in the Mantle and Stratiform Chromitites in the Crust: A Hypothesis. *Minerals* **2021**, *11*, 209. [CrossRef]
2. Naldrett, A.J.; Kinnaird, J.; Wilson, A.; Yudovskaya, M.; McQuade, S.; Chunnnett, G.; Stanley, C. Chromite composition and PGE content of Bushveld chromitites: Part 1—The Lower and Middle Groups. *Trans. Inst. Min. Metal. B Appl. Earth Sci.* **2009**, *118*, 131–161. [CrossRef]
3. Mosier, D.L.; Singer, D.A.; Moring, B.C.; Galloway, J.P. Podiform chromite deposits—Database and grade and tonnage models. *US Geol. Surv. Sci. Investig. Rep.* **2012**, *5157*, 54.
4. Cawthorn, R.G. The Platinum Group Element Deposits of the Bushveld Complex in South Africa. *Platin. Met. Rev.* **2010**, *54*, 205–215. [CrossRef]
5. Dilek, Y.; Furnes, H.; Shallo, M. Suprasubduction zone ophiolite formation along the periphery of Mesozoic Gondwana. *Gond. Res.* **2007**, *11*, 453–475. [CrossRef]

6. Robertson, A.H.F. Overview of the genesis and emplacement of Mesozoic ophiolites in the Eastern Mediterranean Tethyan region. *Lithos* **2002**, *65*, 1–67. [[CrossRef](#)]
7. Dilek, Y.; Furnes, H. Structure and geochemistry of Tethyan ophiolites and their petrogenesis in subduction rollback systems. *Lithos* **2009**, *113*, 1–20. [[CrossRef](#)]
8. Dilek, Y.; Furnes, H. Ophiolite genesis and global tectonics: Geochemical and tectonic fingerprinting of ancient oceanic lithosphere. *Geol. Soc. Am. Bull.* **2011**, *123*, 387–411. [[CrossRef](#)]
9. Zhou, M.-F.; Robinson, P. Origin and tectonic environment of podiform chromite deposits. *Econ. Geol.* **1997**, *92*, 259–262. [[CrossRef](#)]
10. Zhou, M.-F.; Sun, M.; Keays, R.R.; Kerrich, R.W. Controls on platinum-group elemental distributions of podiform chromitites: A case study of high-Cr and high-Al chromitites from Chinese orogenic belts. *Geochim. Cosmochim. Acta* **1998**, *62*, 677–688. [[CrossRef](#)]
11. Zhou, M.-F.; Robinson, P.T.; Malpas, J.; Aitchison, J.; Sun, M.; Baj, W.J.; Hu, X.F.; Yang, J.S. Melt/mantle interaction and melt evolution in the Sartohay high-Al chromite deposits of the Dalabute ophiolite (NW China). *J. Asian Earth Sci.* **2001**, *19*, 517–534. [[CrossRef](#)]
12. Economou-Eliopoulos, M.; Tsoupas, G.; Kiouisis, G. Exploration for platinum-group elements (PGE) in various geotectonic settings of Greece. *J. Virt. Expl.* **2013**, *45*, 65–82.
13. Zaccarini, F.; Economou-Eliopoulos, M.; Kiseleva, O.; Garuti, G.; Tsikouras, B.; Pushkarev, E.; Idrus, A. Platinum Group Elements (PGE) Geochemistry and Mineralogy of Low Economic Potential (Rh-Pt-Pd)-Rich Chromitites from Ophiolite Complexes. *Minerals* **2022**, *12*, 1565. [[CrossRef](#)]
14. Moores, E.M. Origin and emplacement of ophiolites. *Rev. Geophys.* **1982**, *20*, 735–760. [[CrossRef](#)]
15. Bortolotti, V.; Chiari, M.; Marcucci, M.; Marroni, M.; Pandolfi, L.; Principi, G.; Saccani, E. Comparison among the Albanian and Greek ophiolites: In search of constraints for the evolution of the mesozoic Tethys ocean. *Ophioliti* **2004**, *29*, 19–35.
16. Cortesogno, L.; Galbiati, B.; Principi, G. Note alla “Carta geologica delle ofioliti del Bracco” e ricostruzione della paleogeografia Giurassico, Cretacica. *Ophioliti* **1987**, *12*, 261–342.
17. Jacobshagen, V.; Durr, S.; Kockel, F.; Kopp, K.O.; Kowalczyk, G. Structure and geodynamic evolution of the Aegean region. In *Alps, Apennines, Hellenides*; Closs, H., Roeder, D., Schmidt, K., Eds.; Schweizerbart: Stuttgart, Germany, 1978; pp. 537–564.
18. Ketin, İ. Tectonic units of Anatolia (Asia Minor). *Bull. Mineral Res. Expl. Inst. Turkey* **1966**, *66*, 24–37.
19. Parlak, O.; Delaloye, M. Precise <sup>40</sup>Ar/<sup>39</sup>Ar ages from the metamorphic sole of the Mersin ophiolite (southern Turkey). *Tectonophysics* **1999**, *301*, 145–158. [[CrossRef](#)]
20. Hoeck, V.; Koller, F.; Meisel, T.; Onuzi, K.; Kneringer, E. The Jurassic South Albanian ophiolites: MOR- vs. SSZ-type ophiolites. *Lithos* **1992**, *65*, 143–164. [[CrossRef](#)]
21. Baumgartner, R.J.; Zaccarini, F.; Garuti, G.; Thalhammer, O.A.R. Mineralogical and geochemical investigation of layered chromitites from the Bracco-Gabbro complex, Ligurian ophiolite, Italy. *Cont. Mineral. Petrol.* **2013**, *165*, 477–493. [[CrossRef](#)]
22. Çina, A.; Casli, H.; Goci, L. Chromites in the ophiolites of Albanides. In *Cromite*; Petrascheck, W., Karamata, S., Kravchenko, G.G., Johan, J., Economou, M., Engin, T., Eds.; Theophrastus Publication: Athens, Greece, 1986; pp. 107–128.
23. Çina, A.; Neziraj, A.; Karaj, N.; Johan, Z.; Ohnenstetter, M. PGE mineralization related to Albanian ophiolitic complex. *Geol. Carpat.* **2002**, *53*, 1–7.
24. Çina, A. (Ed.) *On Mineralogy and Metallogeny of Albanides*; Polytechnic University of Albania: Tirana, Albania, 2014; pp. 3–478, ISBN 978-9928-181-12-1.
25. Economou, G.; Economou, M. Some chromite occurrences from the areas of Vermio and Veria, Macedonia, Greece. In *Metallogeny of Basic and Ultrabasic Rocks*; Gallagher, M.J., Ixer, R.A., Neary, C.R., Prichard, H.M., Eds.; Institution of Mining and Metallurgy: London, UK, 1986; pp. 351–354.
26. Economou, M.; Dimou, E.; Economou, D.; Migiros, G.; Vacondios, I.; Grivas, E.; Rassios, A.; Dabitzias, S. Chromite deposits of Greece. In *Cromite*; Petrascheck, W., Karamata, S., Kravchenko, G.G., Johan, J., Economou, M., Engin, T., Eds.; Theophrastus Publication: Athens, Greece, 1986; pp. 129–159.
27. Engin, T.; Özkoçak, O.; Artan, U. General geological setting and character of chromite deposits in Turkey. In *Cromite*; Petrascheck, W., Karamata, S., Kravchenko, G.G., Johan, J., Economou, M., Engin, T., Eds.; Theophrastus Publication: Athens, Greece, 1986; pp. 199–228.
28. Jankovic, S.; Karamata, S. The chromite deposits of the NE Mediterranean: Principal morpho-structural features and genetic implications. In *Cromite*; Petrascheck, W., Karamata, S., Kravchenko, G.G., Johan, J., Economou, M., Engin, T., Eds.; Theophrastus Publication: Athens, Greece, 1986; pp. 45–66.
29. Jankovic, S. General features of chromite deposits and major ore district in Yugoslavia. In *Cromite*; Petrascheck, W., Karamata, S., Kravchenko, G.G., Johan, J., Economou, M., Engin, T., Eds.; Theophrastus Publication: Athens, Greece, 1986; pp. 67–89.
30. Obradovic, L.J. On the chemistry of chromitites from Bregoviza, Sara Mountain, Yugoslavia. In *Cromite*; Petrascheck, W., Karamata, S., Kravchenko, G.G., Johan, J., Economou, M., Engin, T., Eds.; Theophrastus Publication: Athens, Greece, 1986; pp. 91–105.
31. Panayiotou, A.; Michaelides, A.E.; Georgiou, E. The chromite deposits of the Troodos ophiolite complex, Cyprus. In *Cromite*; Petrascheck, W., Karamata, S., Kravchenko, G.G., Johan, J., Economou, M., Engin, T., Eds.; Theophrastus Publication: Athens, Greece, 1986; pp. 161–198.

32. Economou-Eliopoulos, M. Platinum-group element (PGE) distribution in chromite ores from ophiolite complexes of Greece: Implications for chromite exploration. *Ofioliti* **1993**, *18*, 83–97.
33. Economou-Eliopoulos, M.; Eliopoulos, D. Significance of a spatial association of high-Cr and high-Al chromitites for their genesis and exploration. *Bull. T. CXIX Acad. Serbe Sci. Arts* **1999**, *39*, 127–140.
34. Economou-Eliopoulos, M. Platinum-group element distribution in chromite ores from ophiolite complexes: Implications for their exploration. *Ore Geol. Rev.* **1996**, *11*, 363–381. [[CrossRef](#)]
35. Beqiraj, A.; Masi, U.; Violo, M. Geochemical characterization of podiform chromite ores from the ultramafic massif of Bulqiza (Eastern Ophiolitic Belt, Albania) and hints for exploration. *Explor. Min. Geol.* **2000**, *9*, 149–156. [[CrossRef](#)]
36. Tashko, A.; Economou-Eliopoulos, M.; Economou, G. An overview of the PGE distribution in the Bulquiza ophiolite complex, Albania. *Bull. Geol. Soc. Greece* **1998**, *32*, 193–201.
37. Qiu, T.; Yang, J.; Milushi, I.; Wu, W.; Mekshiqi, N.; Xiong, F.; Zhang, C.; Shen, T. Petrogenesis and PGE Abundances of High-Cr and High-Al Chromitites and Peridotites from the Bulqiza Ultramafic Massif, Eastern Mirdita Ophiolite, Albania. *Acta Geol. Sin. Engl. Ed.* **2018**, *93*, 25. [[CrossRef](#)]
38. Kocks, H.; Melcher, F.; Meisel, T.; Burgath, K.-P. Diverse contributing sources to chromitite petrogenesis in the Shebenik Ophiolitic Complex, Albania: Evidence from new PGE- and Os-isotope data. *Mineral. Petrol.* **2007**, *91*, 139–170. [[CrossRef](#)]
39. Economou, M. Platinum-group elements (PGE) in chromite and sulfide ores related with ophiolites. Metallogeny of Basic and Ultrabasic Rocks. In *Metallogeny of Basic and Ultrabasic Rocks*; Gallagher, M.J., Ixer, R.A., Neary, C.R., Prichard, H.M., Eds.; Institution of Mining and Metallurgy: London, UK, 1986; pp. 441–453.
40. Economou-Eliopoulos, M.; Vacondios, I. Geochemistry of chromitites and host rocks from the Pindos ophiolite complex, northwestern Greece. *Chem. Geol.* **1995**, *122*, 99–108. [[CrossRef](#)]
41. Tarkian, M.; Economou-Eliopoulos, M.; Sambanis, G. Platinum-group minerals in chromitites from the Pindos ophiolite complex, Greece. *Neues Jahr. Mineral. Monat.* **1996**, *4*, 145–160.
42. Prichard, H.M.; Economou-Eliopoulos, M.; Fisher, P.C. Contrasting platinum-group mineral assemblages from two different podiform chromitite localities in the Pindos ophiolite complex, Greece. *Can. Mineral.* **2008**, *46*, 329–341. [[CrossRef](#)]
43. Kapsiotis, A.; Grammatikopoulos, T.A.; Tsikouras, B.; Hatzipanagiotou, K.; Zaccarini, F.; Garuti, G. Chromian spinel composition and platinum-group element mineralogy of chromitites from the Milia area, Pindos ophiolite complex, Greece. *Can. Mineral.* **2009**, *47*, 1037–1056. [[CrossRef](#)]
44. Kapsiotis, A.; Grammatikopoulos, T.A.; Tsikouras, B.; Hatzipanagiotou, K. Platinum-group mineral characterization in concentrates from high-grade PGE Al-rich chromitites of Korydallos area in the Pindos ophiolite complex (NW Greece). *Res. Geol.* **2010**, *60*, 178–191. [[CrossRef](#)]
45. Economou, M. Platinum group metals in chromite ores from the Vourinos ophiolite complex, Greece. *Ofioliti* **1983**, *8*, 339–355.
46. Talkington, R.W.; Watkinson, D.H. Whole rock platinum-group element trends in chromite-rich rocks in ophiolitic and stratiform igneous complexes. In *Metallogeny of Basic and Ultrabasic Rocks*; Gallagher, M.J., Ixer, R.A., Neary, C.R., Prichard, H.M., Eds.; Institution of Mining and Metallurgy: London, UK, 1986; pp. 427–440.
47. Cocherie, A.; Auge, T.; Meyer, G. Geochemistry of the platinum-group elements in various types of spinels from the Vourinos ophiolitic complex, Greece. *Chem. Geol.* **1989**, *77*, 27–39. [[CrossRef](#)]
48. Konstantopoulou, G.; Economou-Eliopoulos, M. Distribution of platinum-group elements and gold within the Vourinos chromitite ores, Greece. *Econ. Geol.* **1991**, *86*, 1672–1682. [[CrossRef](#)]
49. Grammatikopoulos, T.A.; Kapsiotis, A.; Tsikouras, B.; Hatzipanagiotou, K.; Zaccarini, F.; Garuti, G. Spinel composition, PGE geochemistry and mineralogy of the chromitites from the Vourinos ophiolite complex, northwestern Greece. *Can. Mineral.* **2011**, *49*, 1571–1598. [[CrossRef](#)]
50. Economou, M.; Naldrett, A.J. Sulfides associated with podiform bodies of chromite at Tsagli, Eretria, Greece. *Mineral. Depos.* **1984**, *19*, 289–297. [[CrossRef](#)]
51. Economou-Eliopoulos, M.; Parry, S.J.; Christidis, G. Platinum-group elements (PGE) content of chromite ores from the Othrys ophiolite complex, Greece. In *Mineral Deposits: Research and Exploration Where Do They Meet? Proceedings of the 4th SGA Turku, Finland, 11–13 August 1997*; Papunen, H., Ed.; Balkema: Rotterdam, The Netherlands, 1997; pp. 415–418.
52. Tsoupas, G.; Economou-Eliopoulos, M. High PGE contents and extremely abundant PGE-minerals hosted in chromitites from the Veria ophiolite complex, northern Greece. *Ore Geol. Rev.* **2008**, *33*, 3–19. [[CrossRef](#)]
53. Tarkian, M.; Economou-Eliopoulos, M.; Eliopoulos, D.G. Platinum-Group Minerals and Tetraauricupride in Ophiolitic Rocks of Skyros Island, Greece. *Mineral. Petrol.* **1992**, *47*, 55–66. [[CrossRef](#)]
54. Economou, M. On the chemical composition of the chromite ores from the Chalkidiki peninsula, Greece. *Ofioliti* **1984**, *9*, 123–134.
55. Sideridis, A.; Zaccarini, F.; Koutsovitis, P.; Grammatikopoulos, T.; Tsikouras, B.; Garuti, G.; Hatzipanagiotou, K. Chromitites from the Vavdos ophiolite (Chalkidiki, Greece): Petrogenesis and geotectonic settings; constrains from spinel, olivine composition, PGE mineralogy and geochemistry. *Ore Geol. Rev.* **2021**, *137*, 104289. [[CrossRef](#)]
56. Sideridis, A.; Koutsovitis, P.; Tsikouras, B.; Karkalis, C.; Hauzenberger, C.; Zaccarini, F.; Tsitsanis, P.; Lazaratou, C.V.; Skliros, V.; Panagiotaras, D.; et al. Pervasive Listwaenitization: The Role of Subducted Sediments within Mantle Wedge, W. Chalkidiki Ophiolites, N. Greece. *Minerals* **2022**, *12*, 1000. [[CrossRef](#)]

57. Bussolesi, M.; Grieco, G.; Zaccarini, F.; Cavallo, A.; Tzamos, E.; Storni, N. Chromite compositional variability and associated PGE enrichments in chromitites from the Gomati and Nea Roda ophiolite, Chalkidiki, Northern Greece. *Mineral. Depos.* **2022**, *57*, 1323–1342. [[CrossRef](#)]
58. Sideridis, A.; Tsikouras, B.; Tsitsanis, P.; Koutsovitis, P.; Zaccarini, F.; Hauenberger, C.; Tsikos, A.; Hatzipanagiotou, K. Post-magmatic processes recorded in bimodal chromitites of the East Chalkidiki meta-ultramafic bodies, Gomati and Nea Roda, Northern Greece. *Front. Earth Sci.* **2022**, *10*, 1031239. [[CrossRef](#)]
59. Uysal, I.; Akmaz, R.M.; Saka, S.; Kapsiotis, A. Coexistence of compositionally heterogeneous chromitites in the Antalya-Isparta ophiolitic suite, SW Turkey: A record of sequential magmatic processes in the sub-arc lithospheric mantle. *Lithos* **2016**, *248–251*, 160–174. [[CrossRef](#)]
60. Kozlu, H.; Prichard, H.; Melcher, F.; Fisher, P.; Brough, C.; Stueben, D. Platinum group element (PGE) mineralisation and chromite geochemistry in the Berit ophiolite (Elbistan/Kahramanmaraş), SE Turkey. *Ore Geol. Rev.* **2014**, *60*, 97–111. [[CrossRef](#)]
61. Akmaz, R.M.; Uysal, I.; Saka, S. Compositional variations of chromite and solid inclusions in ophiolitic chromitites from the southeastern Turkey: Implications for chromitite genesis. *Ore Geol. Rev.* **2014**, *58*, 208–224. [[CrossRef](#)]
62. Page, N.J.; Engin, T.; Singer, D.A.; Haffty, J. Distribution of platinum-group elements in the Bati Kef chromite deposit, Guleman-Elazığ area, eastern Turkey. *Econ. Geol.* **1984**, *79*, 177–184. [[CrossRef](#)]
63. Uysal, I.; Kapsiotis, A.; Akmaz, R.M.; Saka, S.; Seitz, H.M. The Guleman ophiolitic chromitites (SE Turkey) and their link to a compositionally evolving mantle source during subduction initiation. *Ore Geol. Rev.* **2018**, *93*, 98–113. [[CrossRef](#)]
64. Yapici, N.; Nğbangandimbo, G.C.S.; Nurlu, N. Geodynamic significance and genesis of chromitites from the Islahiye ophiolite (Gaziantep, SE Anatolia) as constrained by platinum group element (PGE) compositions and mineral chemistry characteristics. *Acta Geochim.* **2022**, *41*, 741–752. [[CrossRef](#)]
65. Uysal, I.; Zaccarini, F.; Garuti, G.; Meisel, T.; Tarkian, M.; Bernhardt, H.J.; Sadiklar, M.B. Ophiolitic chromitites from the Kahramanmaraş area, southeastern Turkey: Their platinum-group elements (PGE) geochemistry, mineralogy and Os-isotope signature. *Ofioliti* **2007**, *32*, 151–161.
66. Avci, E.; Uysal, I.; Akmaz, R.M.; Saka, S. Ophiolitic chromitites from the Kizilyüksek area of the Pozanti-Karsanti ophiolite (Adana, southern Turkey): Implication for crystallization from a fractionated boninitic melt. *Ore Geol. Rev.* **2017**, *90*, 166–183. [[CrossRef](#)]
67. Akbulut, M.; Pikin, O.; Arai, S.; Özgenc, I.; Minareci, F. Base metal (BM) and platinum-group elements (PGE) mineralogy and geochemistry of the Elmaslar chromite deposit (Denizli, SW Turkey): Implications for a local BM and PGE enrichment. *Ofioliti* **2010**, *35*, 1–20.
68. Xiong, F.; Zoheir, B.; Xu, X.; Lenaz, D.; Yang, J. Genesis and high-pressure evolution of the Köyceğiz ophiolite (SW Turkey): Mineralogical and geochemical characteristics of podiform chromitites. *Ore Geol. Rev.* **2022**, *145*, 10912. [[CrossRef](#)]
69. Uysal, I.; Sadiklar, M.B.; Tarkian, M.; Karsli, O.; Aydin, F. Mineralogy and composition of the chromitites and their platinum-group minerals from Ortaca (Muğla-SW Turkey): Evidence for ophiolitic chromitite genesis. *Mineral. Petrol.* **2005**, *83*, 219–242. [[CrossRef](#)]
70. Uysal, I.; Zaccarini, F.; Burhan Sadiklar, M.; Bernhardt, H.J.; Bigi, S.; Garuti, G. Occurrence of rare Ru-Fe-Os-Ir-oxide and associated Platinum-group minerals (PGM) in the chromitite of Muğla ophiolite, SW-Turkey. *Neues Jahrb. Mineral. Abhand.* **2009**, *185*, 323–333. [[CrossRef](#)]
71. Uysal, I.; Tarkian, M.; Sadiklar, M.B.; Zaccarini, F.; Meisel, T.; Garuti, G.; Heidrich, S. Petrology of Al- and Cr-rich ophiolitic chromitites from the Muğla, SW Turkey: Implications from composition of chromite, solid inclusions of platinum-group mineral, silicate, and base-metal mineral, and Os-isotope geochemistry. *Cont. Mineral. Petrol.* **2009**, *158*, 659–674. [[CrossRef](#)]
72. Uysal, I. Petrology of Upper Mantle Peridotite and Ophiolitic Chromitites from the Muğla (SW-Turkey): Implications from Mineral Chemistry, Major–Trace–Rare Earth Elements (REE)–Platinum–Group Elements (PGE) Geochemistry, PGE Mineralogy and Re–Os Isotope Systematics. Ph.D. Thesis, Karadeniz Technical University, Trabzon, Turkey, 2007; p. 449.
73. Uysal, I.; Akmaz, R.M.; Kapsiotis, A.; Demir, Y.; Saka, S.; Avci, E.; Müller, D. Genesis and geodynamic significance of chromitites from the Orhaneli and Harmancik ophiolites (Bursa, NW Turkey) as evidenced by mineralogical and compositional data. *Ore Geol. Rev.* **2015**, *65*, 26–41. [[CrossRef](#)]
74. Dönmez, C.; Keskin, S.; Günay, K.; Çolakoğlu, A.O.; Çiftçi, Y.; Uysal, I.; Türkel, A.; Yildirim, N. Chromite and PGE geochemistry of the Elekdağ ophiolite (Kastamonu, northern Turkey): Implications for deep magmatic processes in a supra-subduction zone setting. *Ore Geol. Rev.* **2014**, *57*, 216–228. [[CrossRef](#)]
75. Uysal, I.; Zaccarini, F.; Sadiklar, M.B.; Tarkian, M.; Thalhammer, O.A.R.; Garuti, G. The podiform chromitites in the Dağköplü and Kavak mines, Eskişehir ophiolite (NW-Turkey): Genetic implications of mineralogical and geochemical data. *Geol. Acta* **2009**, *7*, 351–362.
76. Uysal, I.; Tarkian, M.; Sadiklar, M.B.; Şen, C. Platinum-group-element geochemistry and mineralogy of ophiolitic chromitites from the Kop Mountains, northeastern Turkey. *Can. Mineral.* **2007**, *45*, 355–377. [[CrossRef](#)]
77. Çimen, O.; Toksoy-Köksal, F.; Öztüfekçi-Önal, A.; Aktağ, A. Depleted to refertilized mantle peridotites hosting chromitites within the Tunceli ophiolite, Eastern Anatolia (Turkey): Insights on the back ARC origin. *Ofioliti* **2016**, *41*, 1–20.
78. Prichard, H.M.; Lord, R. Platinum and palladium in the Troodos ophiolite complex, Cyprus. *Can. Mineral.* **1990**, *28*, 607–617.
79. McElduff, B.; Stumpfl, E.F. Platinum-group minerals from the Troodos ophiolite, Cyprus. *Mineral. Petrol.* **1990**, *42*, 211–232. [[CrossRef](#)]

80. Büchl, A.; Brüggmann, G.; Batanova, V.G. Formation of podiform chromitite deposits: Implications from PGE abundances and Os isotopic compositions of chromites from the Troodos complex, Cyprus. *Chem. Geol.* **2004**, *208*, 217–232. [[CrossRef](#)]
81. Piccardo, G.B.; Rampone, E.; Romairone, A. Formation and composition of the oceanic lithosphere of the Ligurian Tethys: Inferences from the Ligurian ophiolites. *Ophioliti* **2002**, *27*, 145–161.
82. Marroni, M.; Molli, G.; Ottria, G.; Pandolfi, L. Tectono-sedimentary evolution of the External Liguride units (Northern Apennines, Italy): Insights in the pre-collisional history of a fossil ocean-continent transition zone. *Geodin. Acta* **2001**, *14*, 307–320. [[CrossRef](#)]
83. Shallo, M.; Dilek, Y. Development of ideas on the origin of Albanian ophiolites. In *Ophiolite Concept and the Evolution of Geological Thought*; Dilek, Y., Newcomb, S., Eds.; The Geological Society of America: Boulder, CO, USA, 2003; Volume 373, pp. 351–363.
84. Saccani, M.; Photiades, A. Petrogenesis and tectonomagmatic significance of volcanic and subvolcanic rocks in the Albanide–Hellenide ophiolitic mélanges. *Isl. Arc* **2005**, *14*, 494–516. [[CrossRef](#)]
85. Robertson, A.H.F.; Karamata, S. The role of subduction-accretion processes in the tectonic evolution of the Mesozoic Tethys in Serbia. *Tectonophysics* **1994**, *234*, 73–94. [[CrossRef](#)]
86. Rassios, A.E.; Dilek, Y. Rotational deformation in the Jurassic Mesohellenic 879 ophiolites, Greece, and its tectonic significance. *Lithos* **2009**, *108*, 207–223. [[CrossRef](#)]
87. Rogkala, A.; Petrounias, P.; Tsikouras, B.; Giannakopoulou, P.P.; Hatzipanagiotou, K. Mineralogical Evidence for Partial Melting and Melt-Rock Interaction Processes in the Mantle Peridotites of Edessa Ophiolite (North Greece). *Minerals* **2019**, *9*, 120. [[CrossRef](#)]
88. Capedri, S.; Venturelli, G.; Bocchi, G.; Dostal, J.; Garuti, G.; Rossi, A. The geochemistry and petrogenesis of an ophiolitic sequence from Pindos, Greece. *Contr. Mineral. Petrol.* **1980**, *74*, 189–200. [[CrossRef](#)]
89. Economou-Eliopoulos, M.; Tarkian, M.; Sambanis, G. On the geochemistry of chromitites from the Pindos ophiolite complex, Greece. *Chemie der Erde Geochem.* **1999**, *59*, 19–31.
90. Rassios, A.; Beccaluva, L.; Bortolotti, V.; Mavrides, A.; Moores, E.M. The Vourinos ophiolitic complex: A field excursion guidebook. *Ophioliti* **1983**, *8*, 275–292.
91. Kapsiotis, A.; Grammaticopoulos, T.A.; Zaccarini, F.; Tsikouras, B.; Garuti, G.; Hatzipanagiotou, K. Platinum-group mineral characterization in concentrates from low-grade PGE chromitites from the Vourinos ophiolite complex, northern Greece. *Trans. Inst. Min. Metal. B Appl. Earth Sci.* **2006**, *115*, 49–57. [[CrossRef](#)]
92. Koutsovitis, P.; Magganas, A. Boninitic and tholeiitic basaltic lavas and dikes from dispersed Jurassic East Othris ophiolitic units, Greece: Petrogenesis and geodynamic implications. *Int. Geol. Rev.* **2016**, *58*, 1983–2006. [[CrossRef](#)]
93. Meinhold, G.; Kostopoulos, D.K. The Circum-Rhodope Belt, northern Greece: Age, provenance, and tectonic setting. *Tectonophysics* **2013**, *595–596*, 55–68. [[CrossRef](#)]
94. Bonev, N.; Marchev, P.; Moritz, R.; Collings, D. Jurassic subduction zone tectonics of the Rhodope Massif in the Thrace region (NE Greece) as revealed by new U–Pb and <sup>40</sup>Ar/<sup>39</sup>Ar geochronology of the Evros ophiolite and high-grade basement rocks. *Gond. Res.* **2015**, *27*, 760–775. [[CrossRef](#)]
95. Parlak, O.; Höck, V.; Kozlu, H.; Delaloye, M. Oceanic crust generation in an island arc tectonic setting, SE Anatolian orogenic belt (Turkey). *Geol. Mag.* **2004**, *141*, 583–603. [[CrossRef](#)]
96. Alparslan, G.; Dilek, Y. Seafloor spreading structure, geochronology, and tectonic evolution of the Küre ophiolite, Turkey: A Jurassic continental backarc basin oceanic lithosphere in southern Eurasia. *Lithosphere* **2017**, *10*, 14–34. [[CrossRef](#)]
97. Parlak, O. The Tauride ophiolites of Anatolia (Turkey): A review. *J. Earth Sci.* **2016**, *27*, 901–934. [[CrossRef](#)]
98. Parlak, O.; Höck, V.; Delaloye, M. The supra-subduction zone Pozanti–Karsanti ophiolite, southern Turkey: Evidence for high-pressure crystal fractionation of ultramafic cumulates. *Lithos* **2002**, *65*, 205–224. [[CrossRef](#)]
99. Sarifakioğlu, E. Petrology and origin of plagiogranites from the Dağküplü (Eskişehir) ophiolite along the Izmir–Ankara–Erzincan suture zone, Turkey. *Ophioliti* **2007**, *32*, 39–51.
100. Sarifakioğlu, E.; Özen, H.; Winchester, J.A. Whole Rock and Mineral Chemistry of Ultramafic-mafic Cumulates from the Orhaneli (Bursa) Ophiolite, NW Anatolia. *Turkish J. Earth Sci.* **2009**, *18*, 55–83. [[CrossRef](#)]
101. Greenbaum, D. The chromitiferous rocks of the Troodos ophiolite complex, Cyprus. *Econ. Geol.* **1977**, *72*, 1175–1194. [[CrossRef](#)]
102. Naldrett, A.J.; Duke, J.M. Pt metals in magmatic sulfide ores. *Science* **1980**, *208*, 1417–1424. [[CrossRef](#)] [[PubMed](#)]
103. Garuti, G.; Fershtater, G.; Bea, F.; Montero, P.G.; Pushkarev, E.V.; Zaccarini, F. Platinum-group element distribution in mafic-ultramafic complexes of central and southern Urals: Preliminary results. *Tectonophysics* **1997**, *276*, 181–194. [[CrossRef](#)]
104. Johan, Z.; Martin, R.F.; Ettler, V. Fluids are bound to be involved in the formation of ophiolitic chromite deposits. *Eur. J. Mineral.* **2017**, *49*, 534–555. [[CrossRef](#)]
105. Leblanc, M. Platinum-group elements and gold in ophiolitic complexes: Distribution and fractionation from mantle to oceanic floor. In *Ophiolite Genesis and Evolution of Oceanic Lithosphere*; Peters, T.J., Ed.; Kluwer Academic Publishers: Dordrecht, The Netherlands, 1991; pp. 231–260.
106. Boudier, F.; Al-Rajhi, A. Structural control on chromite deposits in ophiolites: The Oman case. In *Tectonic Evolution of the Oman Mountain*; Special Publications; Rollinson, H.R., Searle, M.P., Abbasi, I.A., Al-Lazki, A., Al Kindi, M.H., Eds.; The Geological Society of London: London, UK, 2014; Volume 392, pp. 259–273.
107. Boudier, F.; Nicolas, A. Harzburgite and lherzolite subtypes in ophiolitic and oceanic environments. *Earth Planet. Sci. Lett.* **1985**, *76*, 84–92. [[CrossRef](#)]
108. Keays, R.R. The role of komatiitic and picritic magmatism and S-saturation in the formation of ore deposits. *Lithos* **1995**, *34*, 1–18. [[CrossRef](#)]

- 
109. Naldrett, A.J. Platinum-group element deposits. PGE Mineralogy, Geology, Recovery. *Can. Inst. Min. Metall. Spec. Vol.* **1981**, *23*, 197–231.
  110. Barnes, S.J.; Mungall, J.E.; Maier, W.D. Platinum group elements in mantle melts and mantle samples. *Lithos* **2015**, *232*, 395–417. [[CrossRef](#)]

**Disclaimer/Publisher’s Note:** The statements, opinions and data contained in all publications are solely those of the individual author(s) and contributor(s) and not of MDPI and/or the editor(s). MDPI and/or the editor(s) disclaim responsibility for any injury to people or property resulting from any ideas, methods, instructions or products referred to in the content.